Isotope-differential measurement of Xe atomic EDM with a double-species spin maser

K. Asahi[a], in collaboration with
T. Sato[a], Y. Ichikawab[b,a], S. Kojima[a], C. Funayama[a], S. Tanaka[a], Y. Sakamoto[a], Y. Ohtomo[a], C. Hirao[a], M. Chikamori[a], E. Hikota[a], T. Furukawa[c], A. Yoshimi[d], C.P. Bidinosti[e], T. Ino[f], H. Ueno[b], Y. Matsuo[g], T. Fukuyama[h]

[a]Tokyo Tech, [b]RIKEN, [c]TMU, [d]Okayama U., [e]U. Winnipeg, [f]KEK, [g]Hosei U., and [h]Osaka U.

OUTLINE:

1. EDMs and Symmetries
2. Measuring an EDM
3. Spin masing with I = 3/2 spins
4. Present status of the experiment

§ 1 EDMs and Symmetries

$$\text{EDM} \neq 0 \quad \Leftrightarrow \quad \Delta W \equiv W_{\Uparrow\uparrow} - W_{\Uparrow\downarrow} \propto \boldsymbol{\sigma} \cdot \boldsymbol{E} \neq 0$$

Electric field

Spin

● Classically:

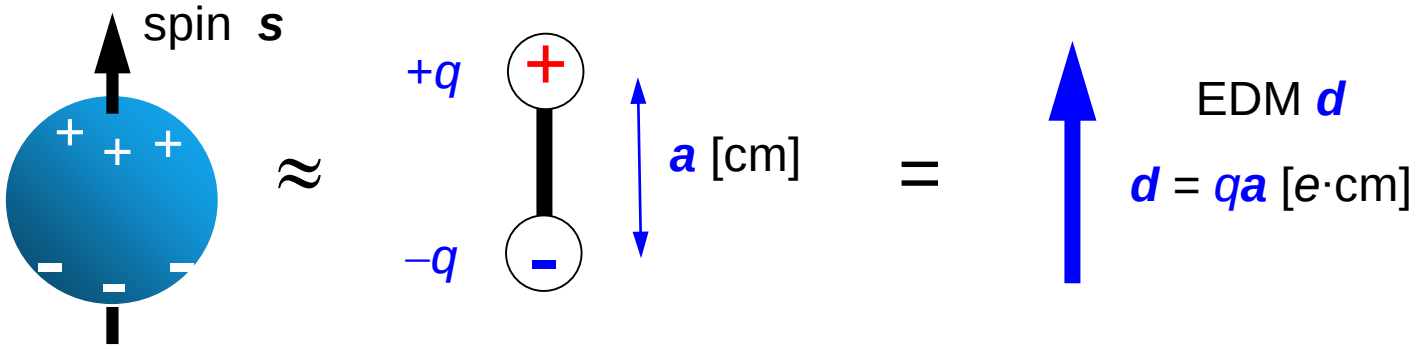

● For elementary fermion:

$$\mathscr{L}_{\text{EDM}} = -\frac{i}{2} d \bar{\psi} \sigma^{\mu\nu} \gamma_5 \psi F_{\mu\nu}$$

Thus... EDM violates T, and hence CP (by CPT theorem)

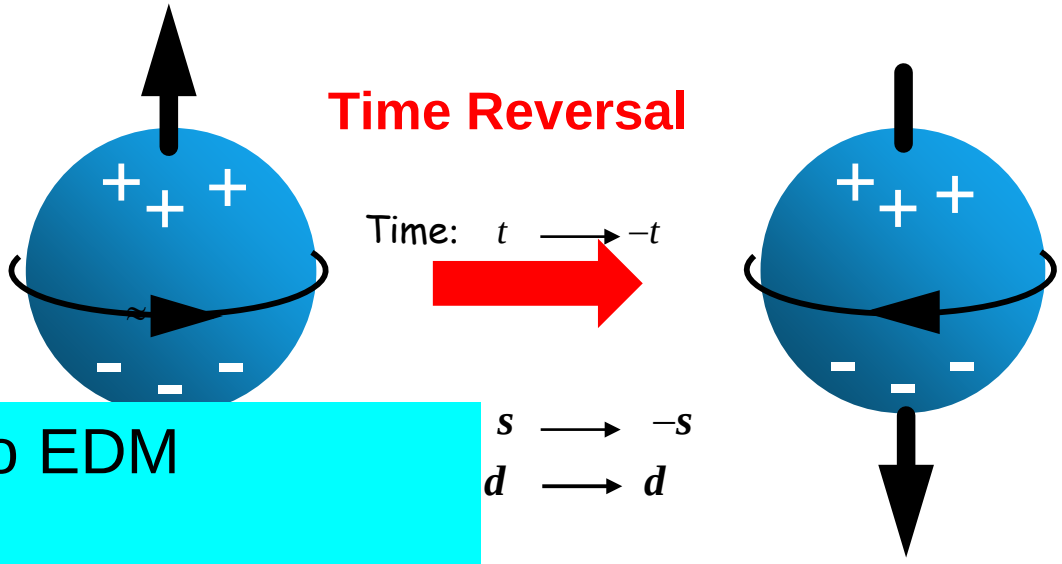

Non-zero EDM
II
Evidence for New Physics

One-loop diagram for EDM

- Standard Model (SM)

  Predicts EDMs that are undetectably small

  -- 10^{-5} times the present limits.

SM

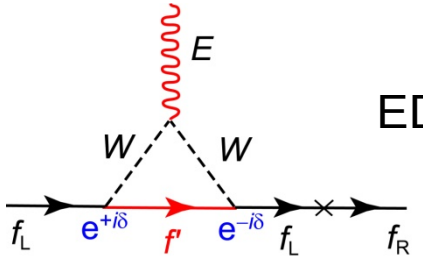

EDM = 0

- Theories beyond the SM

  allow sizes of EDM to be reachable with "a-step-forward" experiments

(e.g.) SUSY

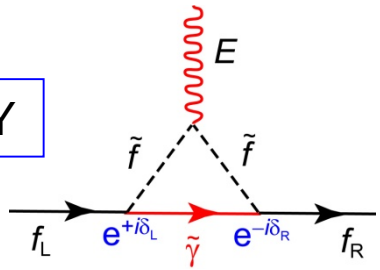

(SM, dim-4)

θ, ϕ_{CKM}

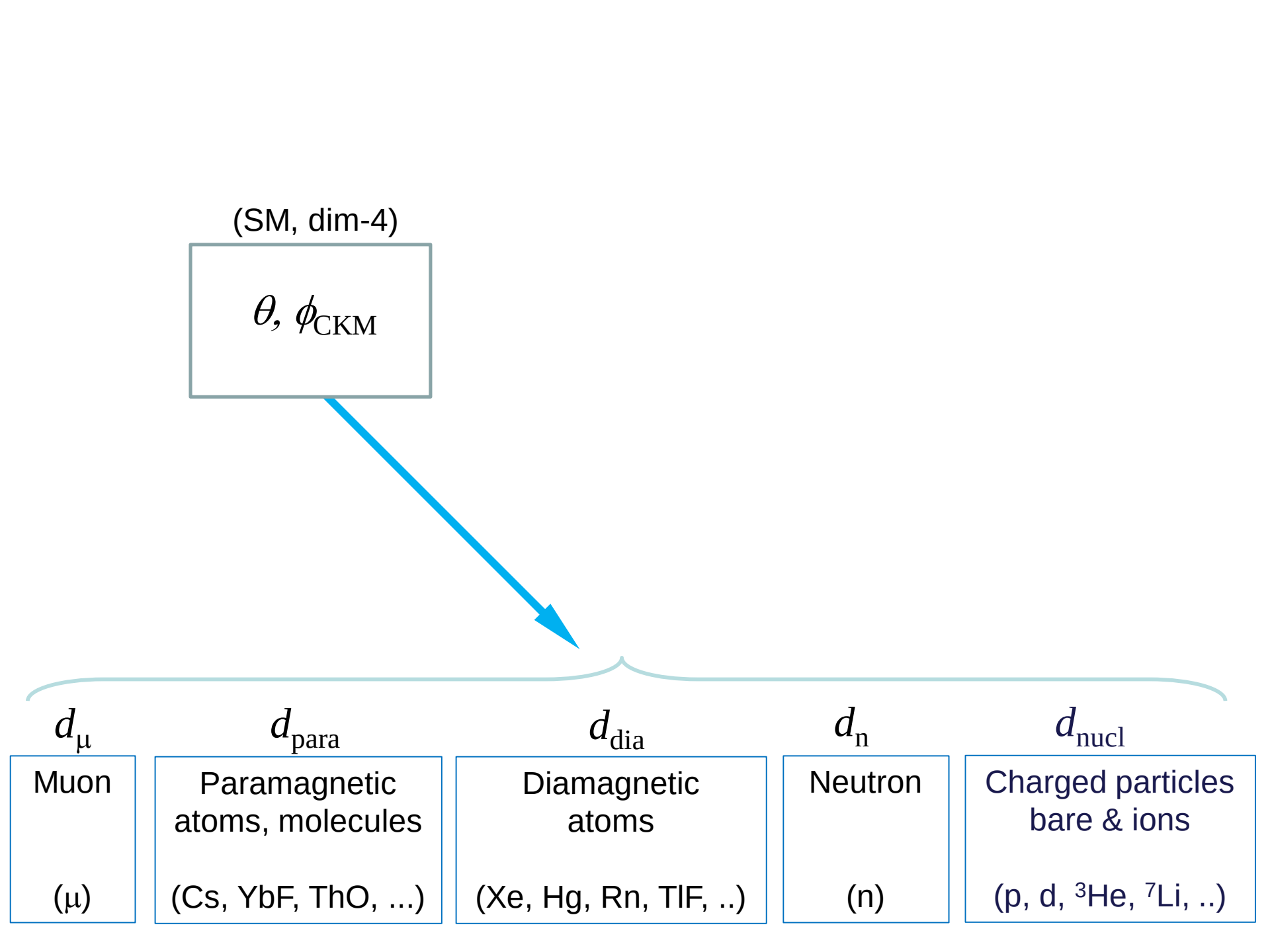

d_μ	d_{para}	d_{dia}	d_n	d_{nucl}
Muon (μ)	Paramagnetic atoms, molecules (Cs, YbF, ThO, ...)	Diamagnetic atoms (Xe, Hg, Rn, TlF, ..)	Neutron (n)	Charged particles bare & ions (p, d, ^{3}He, ^{7}Li, ..)

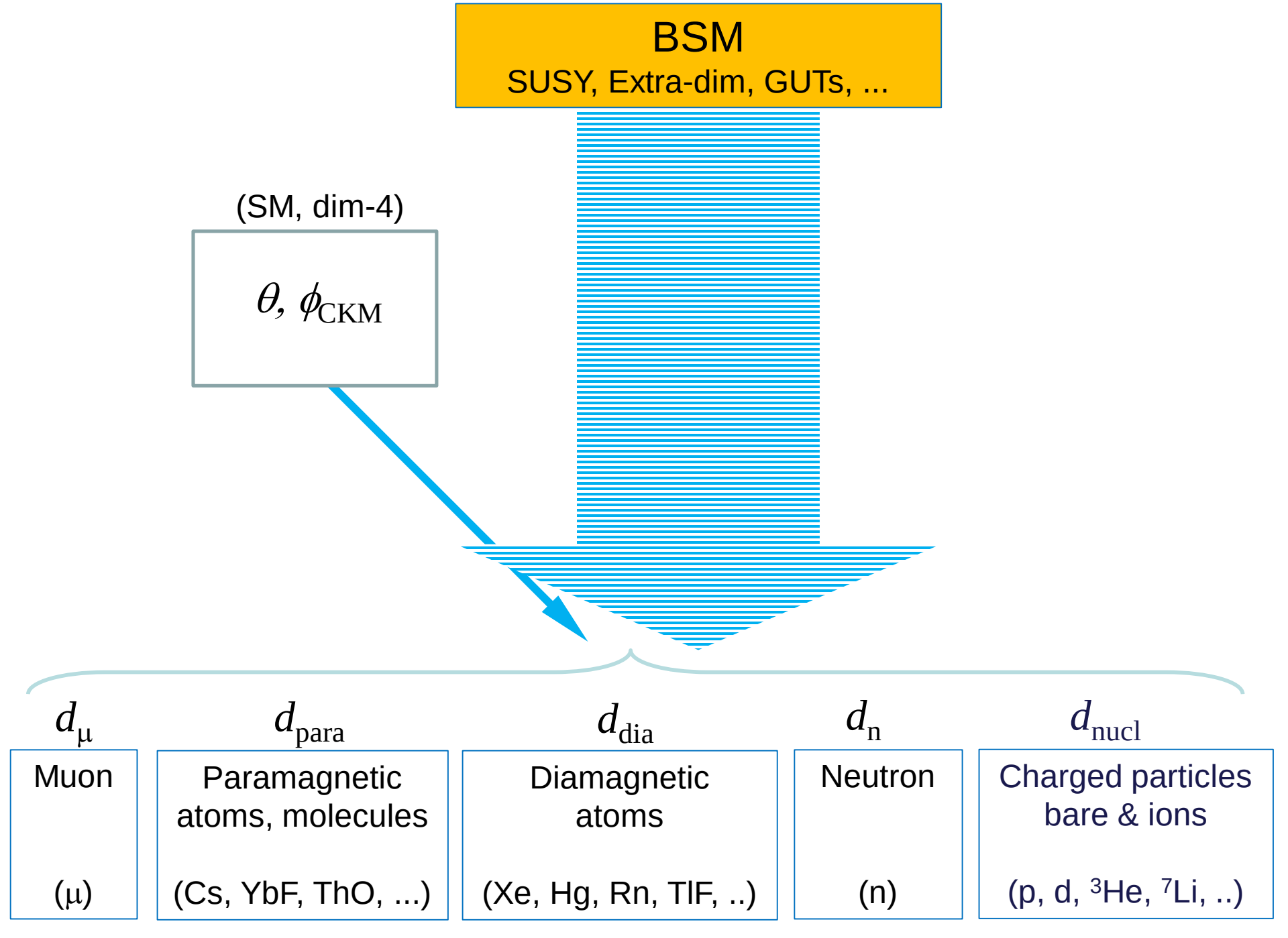
BSM
SUSY, Extra-dim, GUTs, ...
(SM, dim-4)
$\theta, \phi_{\mathrm{CKM}}$
d_{μ}
d_{para}
d_{dia}
d_{n}
d_{nucl}
Muon
(μ)
Paramagnetic atoms, molecules
(Cs, YbF, ThO, ...)
Diamagnetic atoms
(Xe, Hg, Rn, TlF, ..)
Neutron
(n)
Charged particles bare & ions
(p, d, ^{3}He, ^{7}Li, ..)

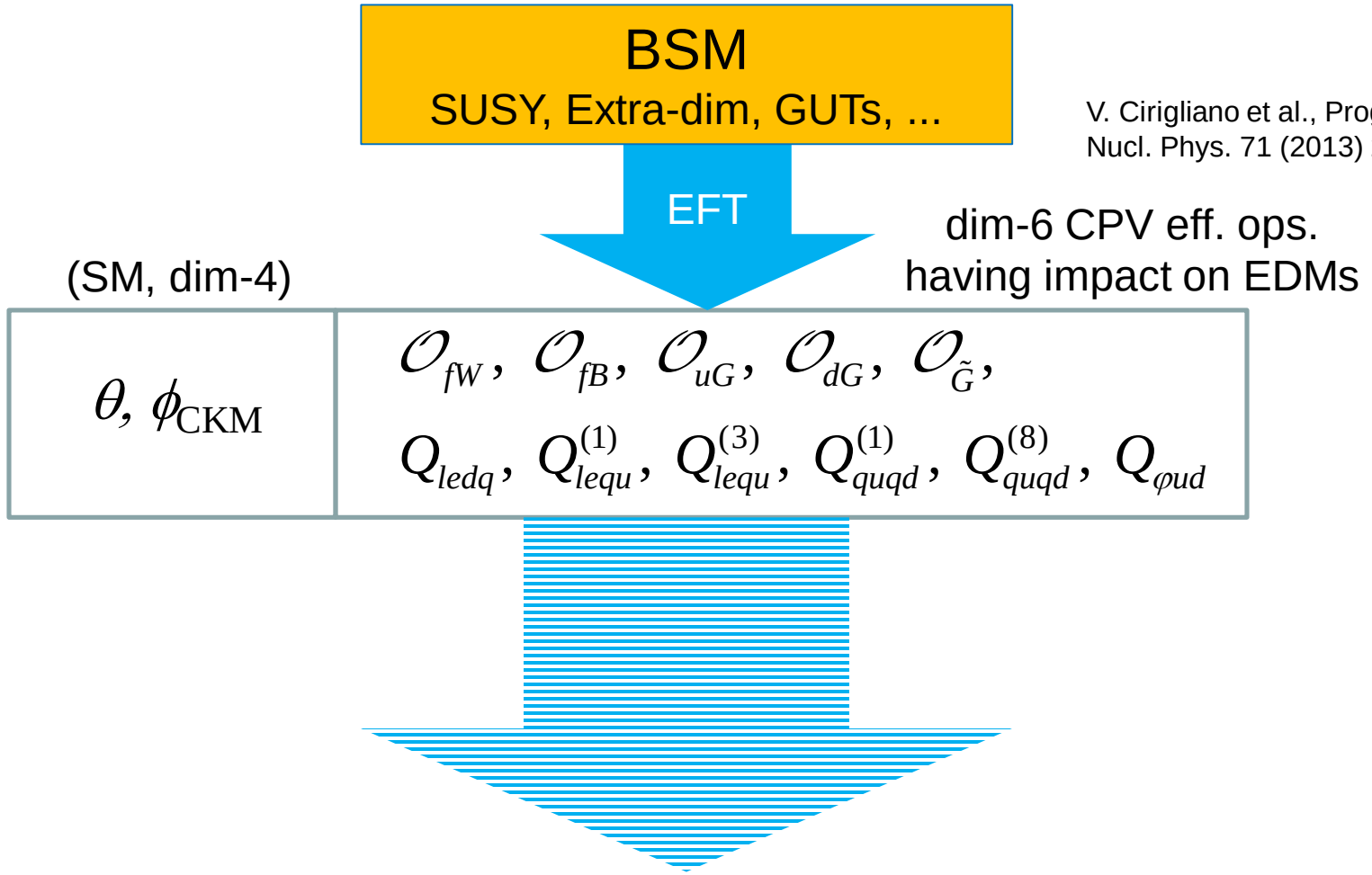
BSM
SUSY, Extra-dim, GUTs, ...
EFT
V. Cirigliano et al., Prog. Part. Nucl. Phys. 71 (2013) 2.
dim-6 CPV eff. ops. having impact on EDMs
(SM, dim-4)
θ, ϕ_{CKM}
$\mathcal{O}_{fW}$, $\mathcal{O}_{fB}$, $\mathcal{O}_{uG}$, $\mathcal{O}_{dG}$, $\mathcal{O}_{\tilde{G}}$,
Q_{ledq}, $Q^{(1)}_{lequ}$, $Q^{(3)}_{lequ}$, $Q^{(1)}_{quqd}$, $Q^{(8)}_{quqd}$, $Q_{\varphi ud}$
d_{μ}
Muon
(μ)
d_{para}
Paramagnetic atoms, molecules
(Cs, YbF, ThO, ...)
d_{dia}
Diamagnetic atoms
(Xe, Hg, Rn, TlF, ..)
d_{n}
Neutron
(n)
d_{nucl}
Charged particles bare & ions
(p, d, ^{3}He, ^{7}Li, ..)

Dim-6 CPV effective operators that are relevant to EDMs

$$\mathcal{L}_{\rm BSM}^{\rm eff} = \frac{1}{\Lambda^2}\sum_i \alpha_i^{(6)}\mathcal{O}_i^{(6)}$$

V. Cirigliano et al., Prog. Part. Nucl. Phys. 71 (2013) 2.

where :

$\mathcal{O}_{\tilde{G}} = f^{abc}\tilde{G}^{a\nu}_{\mu}G^{a\rho}_{\nu}G^{a\mu}_{\rho}$	three-gluon	
$\mathcal{O}_{uG} = \left(\bar{Q}\sigma^{\mu\nu}T^a u_{\rm R}\right)\tilde{\varphi}G^a_{\mu\nu}$	up-quark chromo EDM	dipole
$\mathcal{O}_{dG} = \left(\bar{Q}\sigma^{\mu\nu}T^a d_{\rm R}\right)\varphi G^a_{\mu\nu}$	down-quark chromo EDM	dipole
$\mathcal{O}_{fW} = \left(\bar{F}\sigma^{\mu\nu} f_{\rm R}\right)\tau^I \Phi W^I_{\mu\nu}$	fermion $SU(2)_{\rm L}$ E-W dipole	dipole
$\mathcal{O}_{fB} = \left(\bar{F}\sigma^{\mu\nu} f_{\rm R}\right)\Phi B_{\mu\nu}$	fermion $SU(2)_{\rm L}$ E-W dipole	dipole
$Q_{ledq} = \left(\bar{L}^j e_{\rm R}\right)\left(\bar{d}_{\rm R}Q^j\right)$	CPV semileptonic	four-fermion
$Q^{(1)}_{lequ} = \left(\bar{L}^j e_{\rm R}\right)\varepsilon_{jk}\left(\bar{Q}^k u_{\rm R}\right)$	CPV semileptonic, scaler-scaler	four-fermion
$Q^{(3)}_{lequ} = \left(\bar{L}^j \sigma_{\mu\nu} e_{\rm R}\right)\varepsilon_{jk}\left(\bar{Q}^k \sigma^{\mu\nu} u_{\rm R}\right)$	CPV semileptonic, tensor-tensor	four-fermion
$Q^{(1)}_{quqd} = \left(\bar{Q}^j u_{\rm R}\right)\varepsilon_{jk}\left(\bar{Q}^k d_{\rm R}\right)$	CPV four-quark, singlet-singlet	four-fermion
$Q^{(8)}_{quqd} = \left(\bar{Q}^j T^a u_{\rm R}\right)\varepsilon_{jk}\left(\bar{Q}^k T^a d_{\rm R}\right)$	CPV four-quark, octet-octet	four-fermion
$Q_{\varphi ud} = \mathrm{i}\left(\tilde{\varphi}^{\dagger}D_{\mu}\varphi\right)\bar{u}_{\rm R}\gamma^{\mu}d_{\rm R}$	quark-Higgs	induced four-fermion

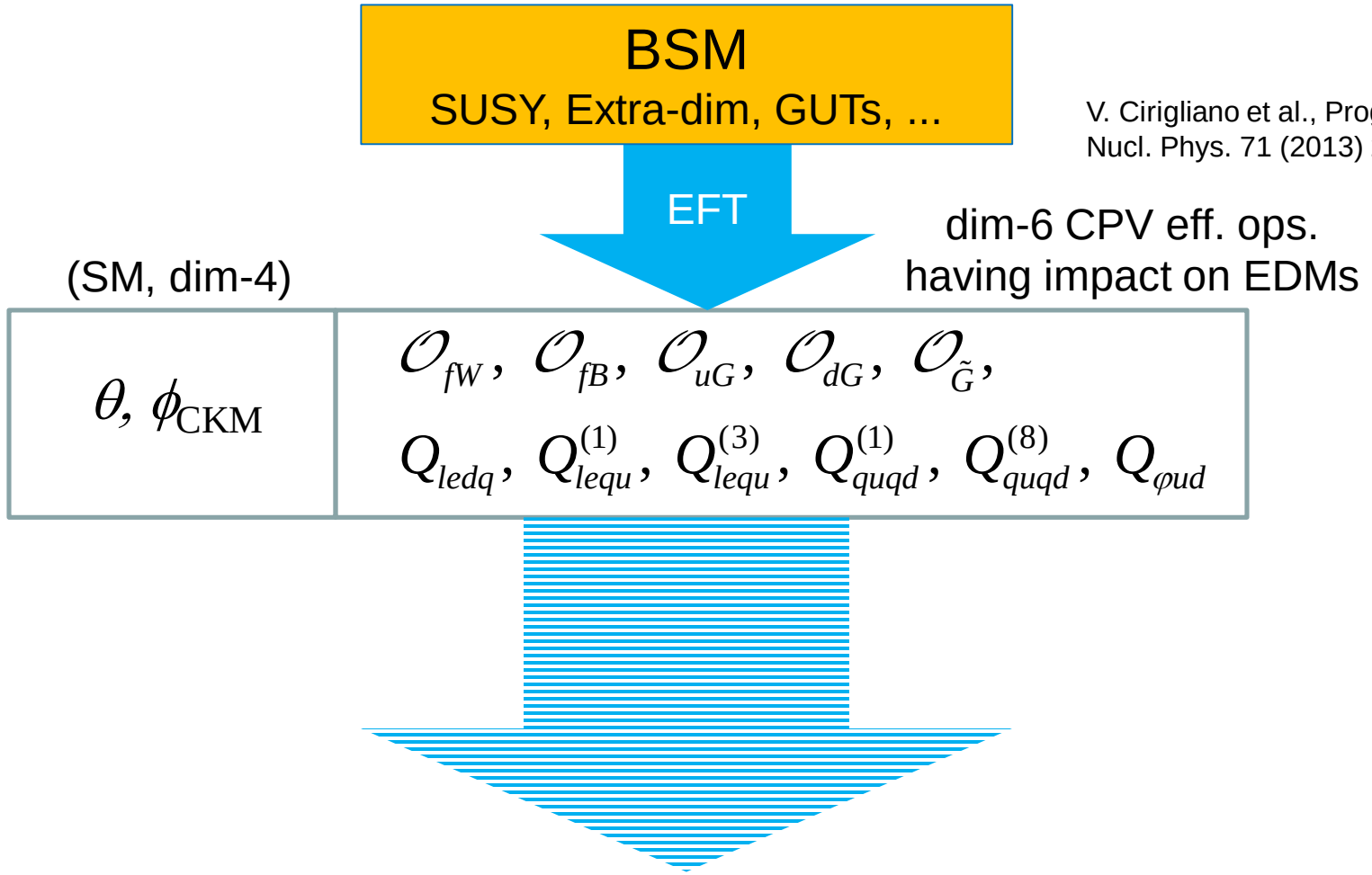
BSM
SUSY, Extra-dim, GUTs, ...
EFT
V. Cirigliano et al., Prog. Part. Nucl. Phys. 71 (2013) 2.
dim-6 CPV eff. ops. having impact on EDMs
(SM, dim-4)
θ, ϕ_{CKM}
$\mathcal{O}_{fW}$, $\mathcal{O}_{fB}$, $\mathcal{O}_{uG}$, $\mathcal{O}_{dG}$, $\mathcal{O}_{\tilde{G}}$,
Q_{ledq}, $Q^{(1)}_{lequ}$, $Q^{(3)}_{lequ}$, $Q^{(1)}_{quqd}$, $Q^{(8)}_{quqd}$, $Q_{\varphi ud}$
d_{μ}
Muon
(μ)
d_{para}
Paramagnetic atoms, molecules
(Cs, YbF, ThO, ...)
d_{dia}
Diamagnetic atoms
(Xe, Hg, Rn, TlF, ..)
d_{n}
Neutron
(n)
d_{nucl}
Charged particles bare & ions
(p, d, ^{3}He, ^{7}Li, ..)

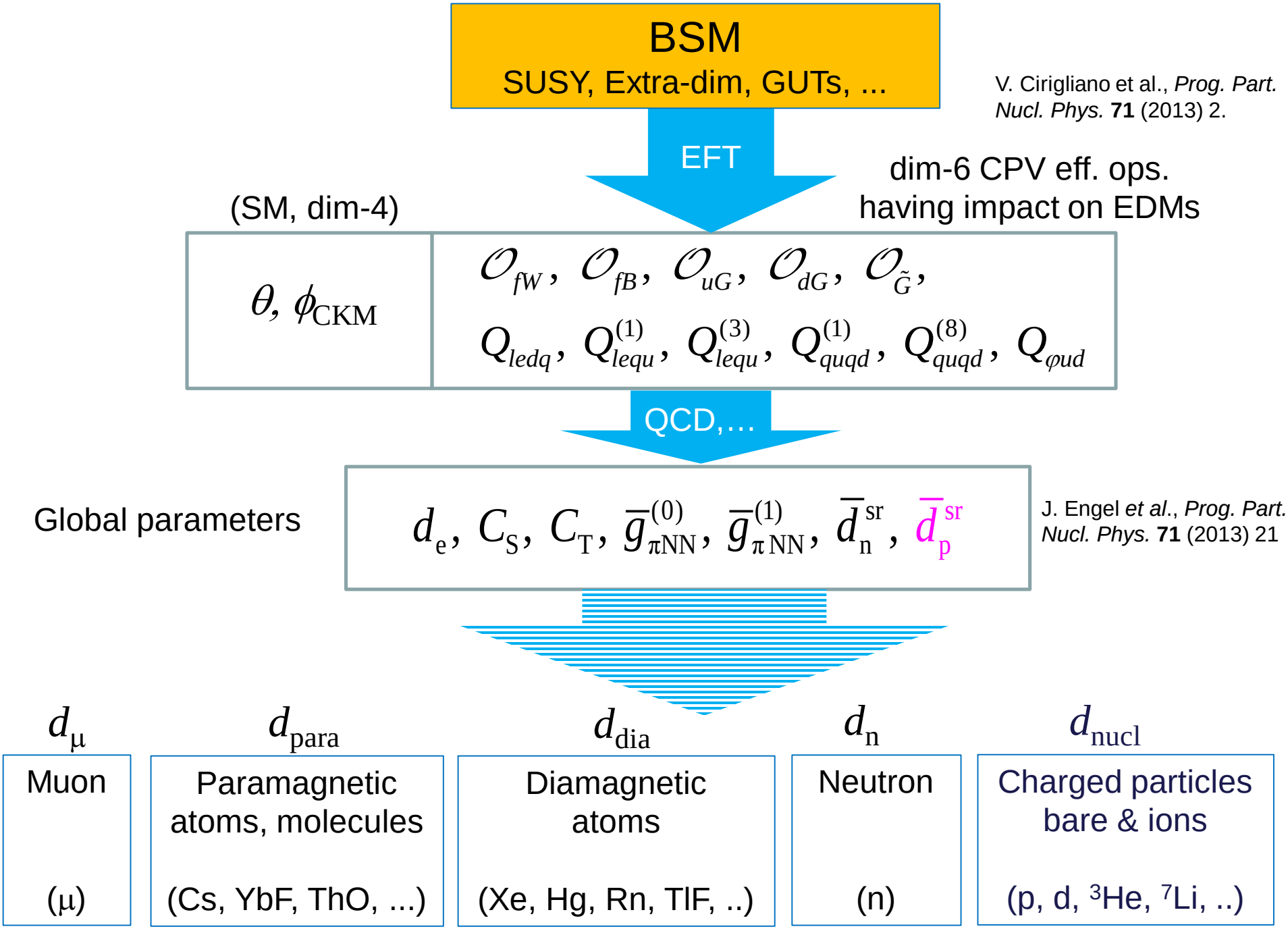
BSM
SUSY, Extra-dim, GUTs, ...
V. Cirigliano et al., Prog. Part. Nucl. Phys. 71 (2013) 2.
EFT
dim-6 CPV eff. ops. having impact on EDMs
(SM, dim-4)
θ, $\phi_{\rm CKM}$
$\mathcal{O}_{fW}$, $\mathcal{O}_{fB}$, $\mathcal{O}_{uG}$, $\mathcal{O}_{dG}$, $\mathcal{O}_{\tilde{G}}$,
Q_{ledq}, $Q^{(1)}_{lequ}$, $Q^{(3)}_{lequ}$, $Q^{(1)}_{quqd}$, $Q^{(8)}_{quqd}$, $Q_{\varphi ud}$
QCD,…
Global parameters
$d_{\rm e}$, $C_{\rm S}$, $C_{\rm T}$, $\bar{g}^{(0)}_{\pi NN}$, $\bar{g}^{(1)}_{\pi NN}$, $\bar{d}^{\rm sr}_{\rm n}$, $\bar{d}^{\rm sr}_{\rm p}$
J. Engel et al., Prog. Part. Nucl. Phys. 71 (2013) 21
d_μ
Muon
(μ)
$d_{\rm para}$
Paramagnetic atoms, molecules
(Cs, YbF, ThO, ...)
$d_{\rm dia}$
Diamagnetic atoms
(Xe, Hg, Rn, TlF, ..)
$d_{\rm n}$
Neutron
(n)
$d_{\rm nucl}$
Charged particles bare & ions
(p, d, ^{3}He, ^{7}Li, ..)

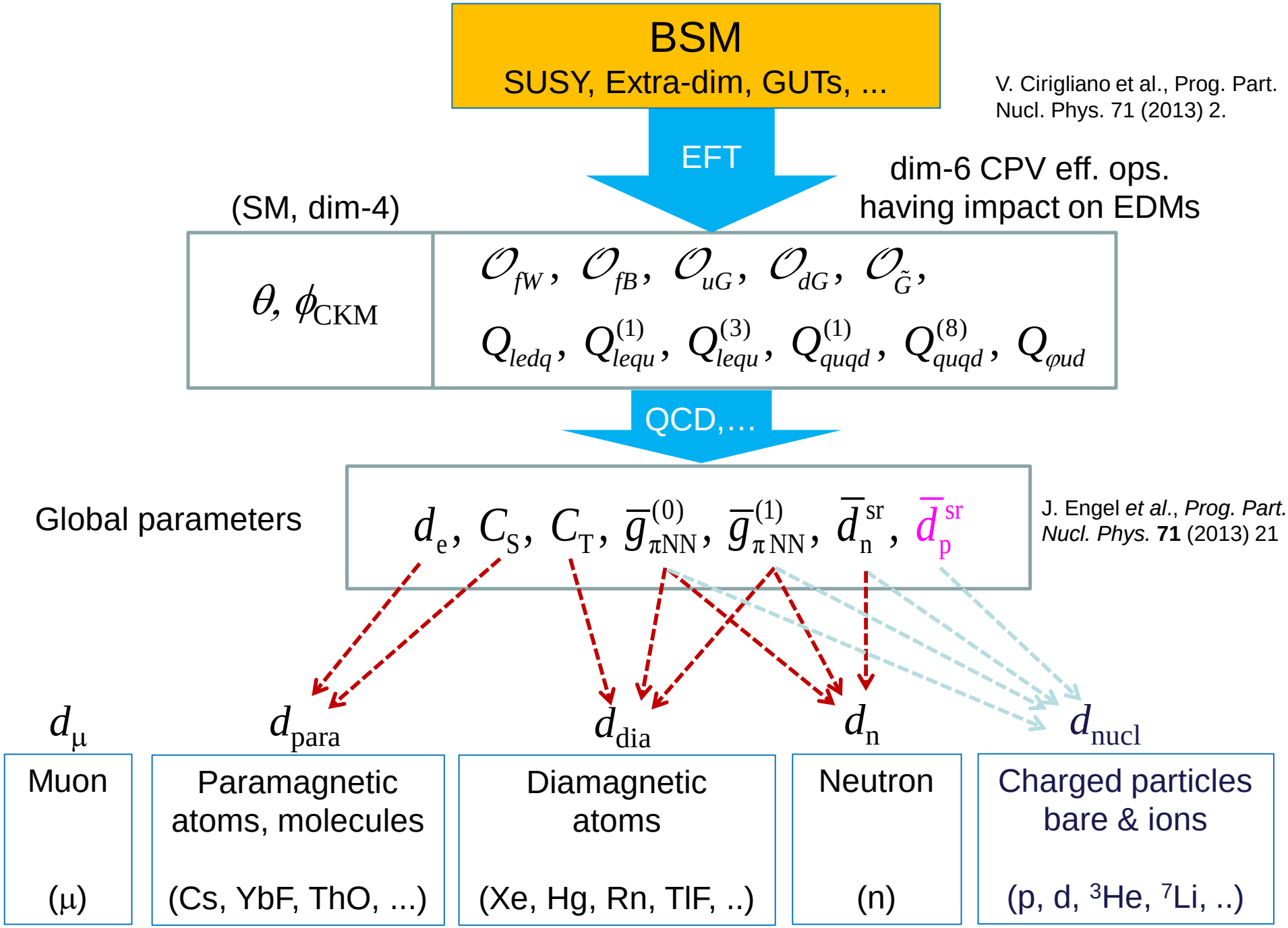
BSM
SUSY, Extra-dim, GUTs, ...
V. Cirigliano et al., Prog. Part. Nucl. Phys. 71 (2013) 2.
EFT
dim-6 CPV eff. ops. having impact on EDMs
(SM, dim-4)
θ, $\phi_{\rm CKM}$
$\mathcal{O}_{fW}$, $\mathcal{O}_{fB}$, $\mathcal{O}_{uG}$, $\mathcal{O}_{dG}$, $\mathcal{O}_{\tilde{G}}$,
Q_{ledq}, $Q^{(1)}_{lequ}$, $Q^{(3)}_{lequ}$, $Q^{(1)}_{quqd}$, $Q^{(8)}_{quqd}$, $Q_{\varphi ud}$
QCD,...
Global parameters
d_e, C_S, C_T, $\bar{g}^{(0)}_{\pi NN}$, $\bar{g}^{(1)}_{\pi NN}$, $\bar{d}^{\rm sr}_n$, $\bar{d}^{\rm sr}_p$
J. Engel et al., Prog. Part. Nucl. Phys. 71 (2013) 21
d_μ
$d_{\rm para}$
$d_{\rm dia}$
d_n
$d_{\rm nucl}$
Muon
(μ)
Paramagnetic atoms, molecules
(Cs, YbF, ThO, ...)
Diamagnetic atoms
(Xe, Hg, Rn, TlF, ..)
Neutron
(n)
Charged particles bare & ions
(p, d, ^{3}He, ^{7}Li, ..)

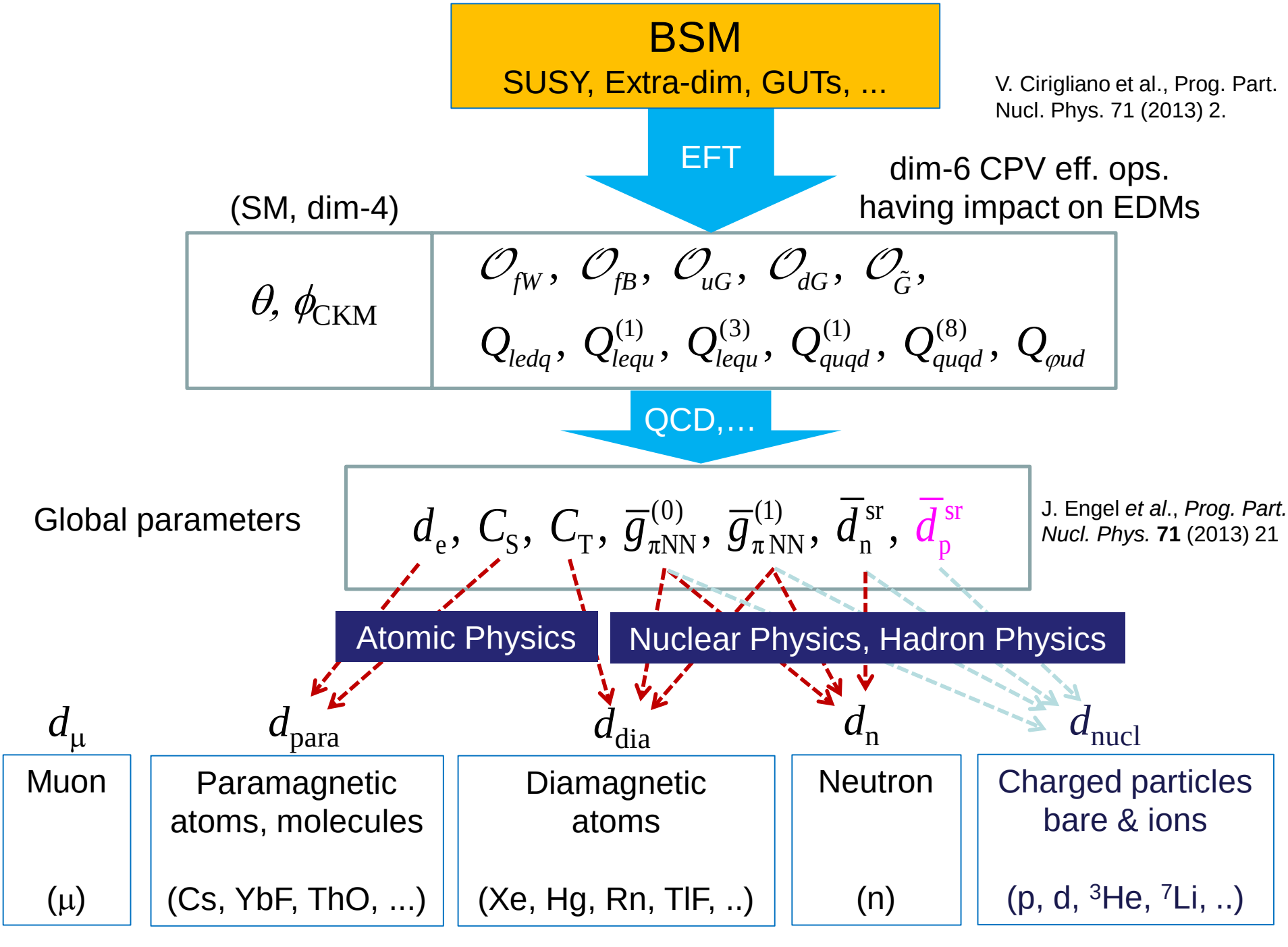
BSM
SUSY, Extra-dim, GUTs, ...
V. Cirigliano et al., Prog. Part. Nucl. Phys. 71 (2013) 2.
EFT
dim-6 CPV eff. ops. having impact on EDMs
(SM, dim-4)
θ, $\phi_{\rm CKM}$
$\mathcal{O}_{fW}$, $\mathcal{O}_{fB}$, $\mathcal{O}_{uG}$, $\mathcal{O}_{dG}$, $\mathcal{O}_{\tilde{G}}$,
Q_{ledq}, $Q^{(1)}_{lequ}$, $Q^{(3)}_{lequ}$, $Q^{(1)}_{quqd}$, $Q^{(8)}_{quqd}$, $Q_{\varphi ud}$
QCD,...
Global parameters
d_e, C_S, C_T, $\bar{g}^{(0)}_{\pi NN}$, $\bar{g}^{(1)}_{\pi NN}$, $\bar{d}^{sr}_n$, $\bar{d}^{sr}_p$
J. Engel et al., Prog. Part. Nucl. Phys. 71 (2013) 21
Atomic Physics
Nuclear Physics, Hadron Physics
d_μ
$d_{\rm para}$
$d_{\rm dia}$
d_n
$d_{\rm nucl}$
Muon
(μ)
Paramagnetic atoms, molecules
(Cs, YbF, ThO, ...)
Diamagnetic atoms
(Xe, Hg, Rn, TlF, ..)
Neutron
(n)
Charged particles bare & ions
(p, d, ^{3}He, ^{7}Li, ..)

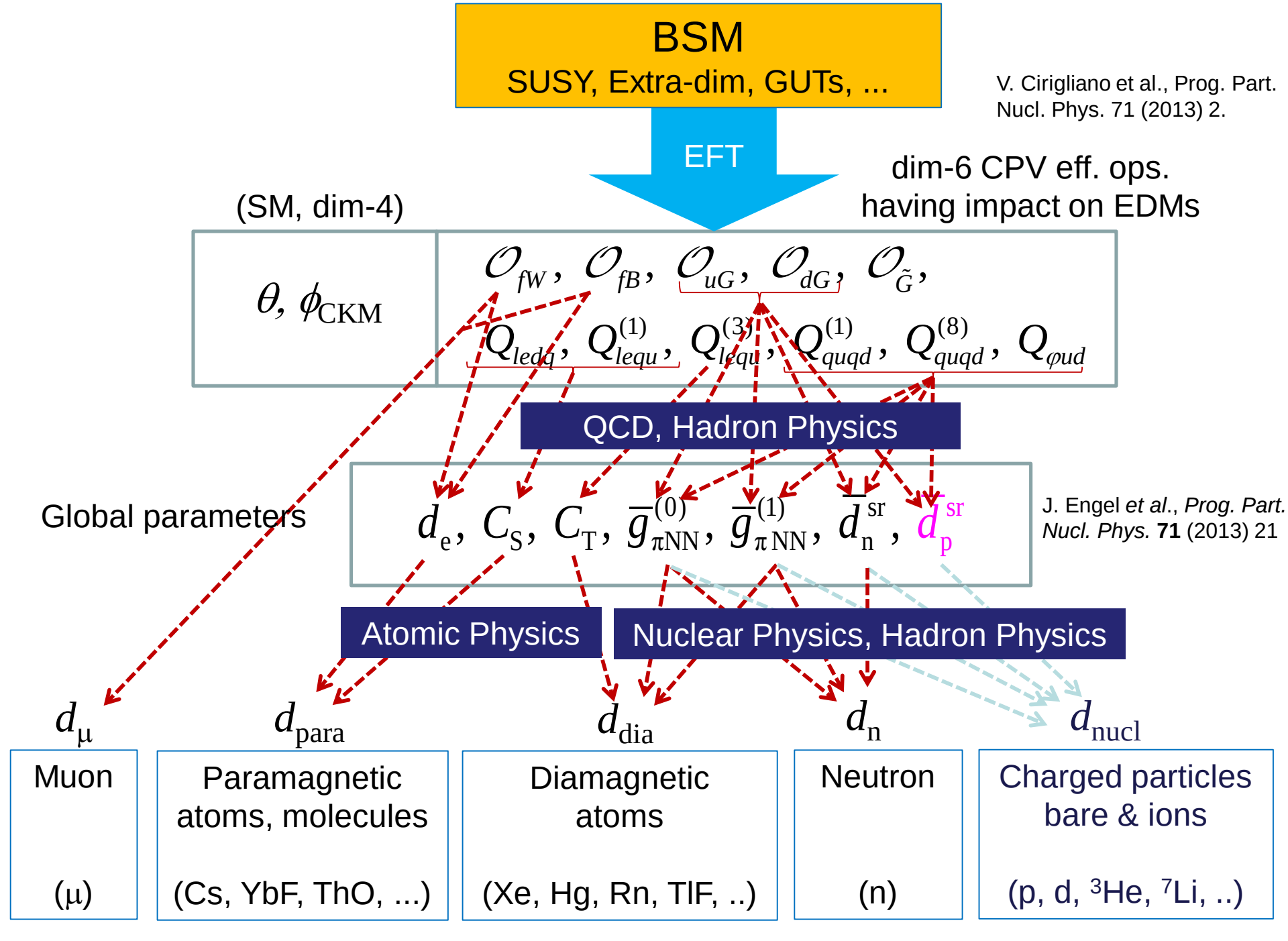
BSM
SUSY, Extra-dim, GUTs, ...
V. Cirigliano et al., Prog. Part. Nucl. Phys. 71 (2013) 2.
EFT
dim-6 CPV eff. ops. having impact on EDMs
(SM, dim-4)
θ, $\phi_{\rm CKM}$
$\mathcal{O}_{fW}$, $\mathcal{O}_{fB}$, $\mathcal{O}_{uG}$, $\mathcal{O}_{dG}$, $\mathcal{O}_{\tilde{G}}$,
Q_{ledq}, $Q^{(1)}_{lequ}$, $Q^{(3)}_{lequ}$, $Q^{(1)}_{quqd}$, $Q^{(8)}_{quqd}$, $Q_{\varphi ud}$
QCD, Hadron Physics
Global parameters
d_e, C_S, C_T, $\bar{g}^{(0)}_{\pi NN}$, $\bar{g}^{(1)}_{\pi NN}$, $\bar{d}^{\rm sr}_n$, $\bar{d}^{\rm sr}_p$
J. Engel et al., Prog. Part. Nucl. Phys. 71 (2013) 21
Atomic Physics
Nuclear Physics, Hadron Physics
d_μ
$d_{\rm para}$
$d_{\rm dia}$
d_n
$d_{\rm nucl}$
Muon
(μ)
Paramagnetic atoms, molecules
(Cs, YbF, ThO, ...)
Diamagnetic atoms
(Xe, Hg, Rn, TlF, ..)
Neutron
(n)
Charged particles bare & ions
(p, d, ^{3}He, ^{7}Li, ..)

Present status of EDM experiments in the World

Particle Species		Source of CPV	Group Name	Recent Result
Neutron	n	d_q, d_q^{color}	ILL (Grenoble) PSI (Zurich) SNS (Oak Ridge) KEK-RCNP-TRIUMF	$\|d_n\| < 2.9 \times 10^{-26}\ e \cdot \text{cm}$ (90% CL)
Diamagnetic Atom	^{199}Hg ^{129}Xe ^{225}Ra ^{A}Rn	d_q, d_q^{color}	Seattle TIT, Princeton, Mainz, Michigan Argonne Rn EDM Collaboration	$\|d_{Hg}\| < 3.1 \times 10^{-29}\ e \cdot \text{cm}$ (95% CL) $\|d_{Ra}\| < 5.0 \times 10^{-22}\ e \cdot \text{cm}$ (95% CL)
Diamagnetic Molecule	TlF YbHg	d_q, d_q^{color}	Hinds (Yale) *et al.* Kyoto U.	
Paramagnetic Atom	Cs Tl Fr	d_e	Amherst Berkeley CYRIC (Tohoku U.)	
Paramagnetic Molecule	YbF ThO PbO PbF	d_e	Hinds (Imperial College London) ACME Collaboration DeMille (Yale) Shafer-Ray (Oklahoma) et al.	$\|d_e\| < 1.05 \times 10^{-27} e \cdot \text{cm}$ (90% CL) $\|d_e\| < 8.7 \times 10^{-29}\ e \cdot \text{cm}$ (90% CL)
Charged Particle	muon proton deuteron	d_μ d_q d_q, d_q^{color}	FNAL, J-PARC, PSI FNAL FNAL	

Based on Table 3 in:
T. Fukuyama, *Int. J. Mod. Phys.* A **27** (2012) 1230015.

The currently most constraining EDMs:

Particle	Result
ThO	$8.7 \times 10^{-29}\ e\mathrm{cm}$
Hg	$3.1 \times 10^{-29}\ e\mathrm{cm}$
Neutron	$2.9 \times 10^{-26}\ e\mathrm{cm}$

Global fit

[T. Chupp and M. Ramsey-Musolf, *Phys. Rev.* C **91** (2015) 035502]

Parameter	Upper Limit (95 % C.L.)
d_e	$5.4 \times 10^{-27}\ e\text{cm}$
C_S	4.5×10^{-7}
C_T	2×10^{-6}
$\bar{g}_{\pi NN}^{(0)}$	8×10^{-9}
$\bar{g}_{\pi NN}^{(1)}$	1×10^{-9}
$\bar{d}_n^{\,\mathrm{sr}}$	12×10^{-23}

Diamagnetic atoms, molecules

(= systems with electron spins being paired off, or without the electron cloud)

$$d_{\rm dia} = \alpha_{S_{\rm Sch}} S_{\rm Sch} + \alpha_{d_{\rm p}} d_{\rm p} + \alpha_{d_{\rm n}} d_{\rm n} + \alpha_{C_{\rm T}^{(0)}} C_{\rm T}^{(0)} + \alpha_{C_{\rm T}^{(1)}} C_{\rm T}^{(1)}$$

● Schiff moment $S_{\rm Sch}$

$$\boldsymbol{S}_{\rm Sch} = \frac{e}{10}\sum_{i=1}^{Z}\left(r_i^2 - \frac{5}{3}\left\langle r^2 \right\rangle_{\rm ch}\right)\boldsymbol{r}_i$$

$$S_{\rm Sch} \equiv \left\langle {\rm g.s.}\middle| S_{\rm Sch}^z \middle| {\rm g.s.}\right\rangle = \frac{m_N g_{\rm A}}{F_\pi}\left(a_0 \bar{g}_{\pi NN}^{(0)} + a_1 \bar{g}_{\pi NN}^{(1)}\right)$$

● Nucleon EDM

$$d_n = \bar{d}_n^{\rm sr} - \frac{e g_{\rm A} \bar{g}_{\pi NN}^{(0)}}{8\pi^2 F_\pi}\left\{ \ln\frac{m_\pi^2}{m_N^2} - \frac{\pi m_\pi}{2m_N} + \frac{\bar{g}_{\pi NN}^{(1)}}{4\bar{g}_{\pi NN}^{(0)}}\left(\kappa_1 - \kappa_0\right)\frac{m_\pi^2}{m_N^2}\ln\frac{m_\pi^2}{m_N^2}\right\}$$

$$d_p = \bar{d}_p^{\rm sr} + \frac{e g_{\rm A} \bar{g}_{\pi NN}^{(0)}}{8\pi^2 F_\pi}\left\{ \ln\frac{m_\pi^2}{m_N^2} - \frac{2\pi m_\pi}{m_N} - \frac{\bar{g}_{\pi NN}^{(1)}}{4\bar{g}_{\pi NN}^{(0)}}\left[\frac{2\pi m_\pi}{m_N} + \left(\frac{5}{2} + \kappa_0 + \kappa_1\right)\frac{m_\pi^2}{m_N^2}\ln\frac{m_\pi^2}{m_N^2}\right]\right\}$$

$\mathcal{O}_{fW}$, $\mathcal{O}_{fB}$ $\rightarrow$ d_q $\rightarrow$ $\bar{d}_p^{\rm sr}$, $\bar{d}_n^{\rm sr}$

$\mathcal{O}_{uG}$, $\mathcal{O}_{dG}$ $\rightarrow$ $\tilde{d}_q$ $\rightarrow$ $g_{\pi NN}^{(0)}$, $g_{\pi NN}^{(1)}$, $g_{\pi NN}^{(2)}$

$Q_{quqd}^{(1)}$, $Q_{quqd}^{(8)}$

$Q_{lequ}^{(3)}$ $\rightarrow$ $C_{\rm T}^{(0)}$, $C_{\rm T}^{(1)}$

● Nuclear spin-dependent e-N PVTV int.

$$\mathcal{L}_{eN}^{\rm NSD} = \frac{8G_{\rm F}}{\sqrt{2}}\bar{e}\sigma_{\mu\nu}ev_N^\nu \bar{N}\left[C_{\rm T}^{(0)} + C_{\rm T}^{(1)}\tau_3\right]S_N^\mu N + \cdots$$

$$\hat{H}_{\rm T} = \frac{2{\rm i}G_{\rm F}}{\sqrt{2}}\delta(\boldsymbol{r})\left[C_{\rm T}^{(0)} + C_{\rm T}^{(1)}\tau_3\right]\boldsymbol{\sigma}_N\cdot\boldsymbol{\gamma}$$

Sensitivity to global CPV parameters

Coefficient values, from the compilation of:
[J. Engel *et al.*, *Prog. Part. Nucl. Phys.* **71** (2013) 21]

$$d_{\mathrm{Hg}} = -\left(0.38^{+2.3}_{-0.19}\times10^{-17}\right)\cdot\bar{g}^{(0)}_{\pi NN} + \left(0^{+1.6}_{-4.9}\times10^{-17}\right)\cdot\bar{g}^{(1)}_{\pi NN} - \left(2.0^{+3.9}_{-0.0}\times10^{-20}\right)\cdot C_{\mathrm{T}}$$

$$d_{\mathrm{Xe}} = -\left(0.29^{+2.3}_{-0.11}\times10^{-18}\right)\cdot\bar{g}^{(0)}_{\pi NN} - \left(0.22^{+1.7}_{-0.11}\times10^{-18}\right)\cdot\bar{g}^{(1)}_{\pi NN} + \left(4^{+2}_{-0}\times10^{-21}\right)\cdot C_{\mathrm{T}}$$

$$d_{\mathrm{n}} = -\left(1.5\times10^{-14}\right)\cdot\bar{g}^{(0)}_{\pi NN} + \left(1.4\times10^{-16}\right)\cdot\bar{g}^{(1)}_{\pi NN}$$

d_{n} : No contribution from C_{T}

d_{Hg} : Vanishingly small contribution from $\bar{g}^{(1)}_{\pi NN}$

- Thus, even though the experimental limits on d(Hg) and d_{n} are already quite severe, the parameters C_{T}, $\bar{g}^{(0)}_{\pi\mathrm{NN}}$, $\bar{g}^{(1)}_{\pi\mathrm{NN}}$ have not been confined much! → d(Xe) needed!!

Coefficients from: [J. Engel *et al.*, *Prog. Part. Nucl. Phys.* **71** (2013) 21]

Analysis from: [T. Chupp and M. Ramsey-Musolf, *Phys. Rev.* C **91** (2015) 035502]

- $\bar{g}_{\pi NN}^{(0)} \approx (-0.01)^{+0.04}_{-0.02} \cdot \left(\frac{v}{\Lambda}\right)^2 \mathrm{Im}\, C_{qG} = (-2)^{+8}_{-4} \times 10^{-7} \cdot \left(\frac{v}{\Lambda}\right)^2 \tilde{\delta}_q$ $< 8 \times 10^{-9}$

  $\tilde{\delta}_q \sim \frac{\alpha_s}{4\pi} \cdot \sin\phi_{\mathrm{CPV}} \rightarrow \boxed{\Lambda > 2\ \mathrm{TeV} \times \sqrt{\sin\phi_{\mathrm{CPV}}}}$

- $\bar{g}_{\pi NN}^{(1)} \approx (-0.02)^{+0.01}_{-0.05} \cdot \left(\frac{v}{\Lambda}\right)^2 \mathrm{Im}\, C_{qG} = (-4)^{+2}_{-10} \times 10^{-7} \cdot \left(\frac{v}{\Lambda}\right)^2 \tilde{\delta}_q$ $< 1 \times 10^{-9}$

- $d_e = (1.13 \times 10^{-16}\, e\mathrm{cm}) \cdot \left(\frac{v}{\Lambda}\right)^2 \mathrm{Im}\, C_{e\gamma} = (3.3 \times 10^{-22}\, e\mathrm{cm}) \cdot \left(\frac{v}{\Lambda}\right)^2 \delta_e$ $< 5.4 \times 10^{-27}\, e\mathrm{cm}$

  $\delta_e \sim \frac{\alpha}{4\pi} \cdot \sin\phi_{\mathrm{CPV}} \rightarrow \boxed{\Lambda > 1.5\ \mathrm{TeV} \times \sqrt{\sin\phi_{\mathrm{CPV}}}}$

- $C_{\mathrm{S}} \approx C_{\mathrm{S}}^{(0)} = -(6.3 \pm 0.8) \cdot \left(\frac{v}{\Lambda}\right)^2 \mathrm{Im}\left(C_{lelq} - C_{lequ}^{(1)}\right)$ $< 4.5 \times 10^{-7}$

  $\mathrm{Im}\left(C_{lelq} - C_{lequ}^{(1)}\right) \sim 1 \rightarrow \boxed{\Lambda > 920\ \mathrm{TeV} \times \sqrt{\sin\phi_{\mathrm{CPV}}}}$

- $C_{\mathrm{T}} \approx C_{\mathrm{T}}^{(0)} = -(0.45 \pm 0.15) \cdot \left(\frac{v}{\Lambda}\right)^2 \mathrm{Im}\, C_{lequ}^{(3)}$ $< 2 \times 10^{-6}$

§ 2 Measuring an EDM

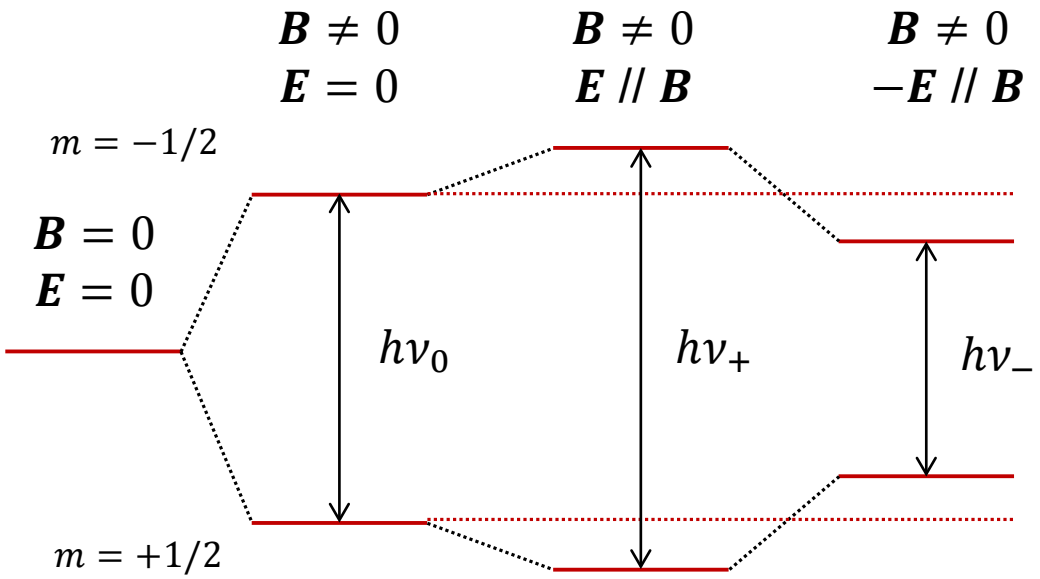

$$H = -\boldsymbol{\mu}\cdot\mathbf{B} - \mathbf{d}\cdot\mathbf{E}$$

$(\mu > 0, d > 0)$

$$E = -\mu B - dE$$

$$\nu_+ = \frac{2\mu B + 2dE}{h}$$

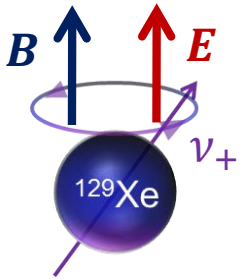

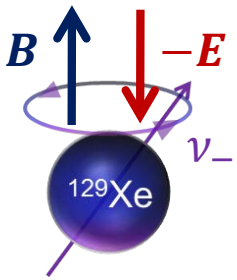

$$E = -\mu B + dE$$

$$\nu_- = \frac{2\mu B - 2dE}{h}$$

$$\Delta\nu = \nu_+ - \nu_- = \frac{4dE}{h}$$

$d = 10^{-26}$ ecm, $E = 100$ kV/cm ⇒ Required frequency precision $\Delta\nu = 1$ μHz

^{129}Xe atomic EDM measurement

- **EDM for a diamagnetic atom ^{129}Xe**
- **External-feedback spin maser**
  - Optical detection of spin
  - Long-term

A. Yoshimi *et al.*, Phys. Lett. A 304 (2002) 13.
A. Yoshimi *et al.*, Phys. Lett. A 376 (2012) 1924.

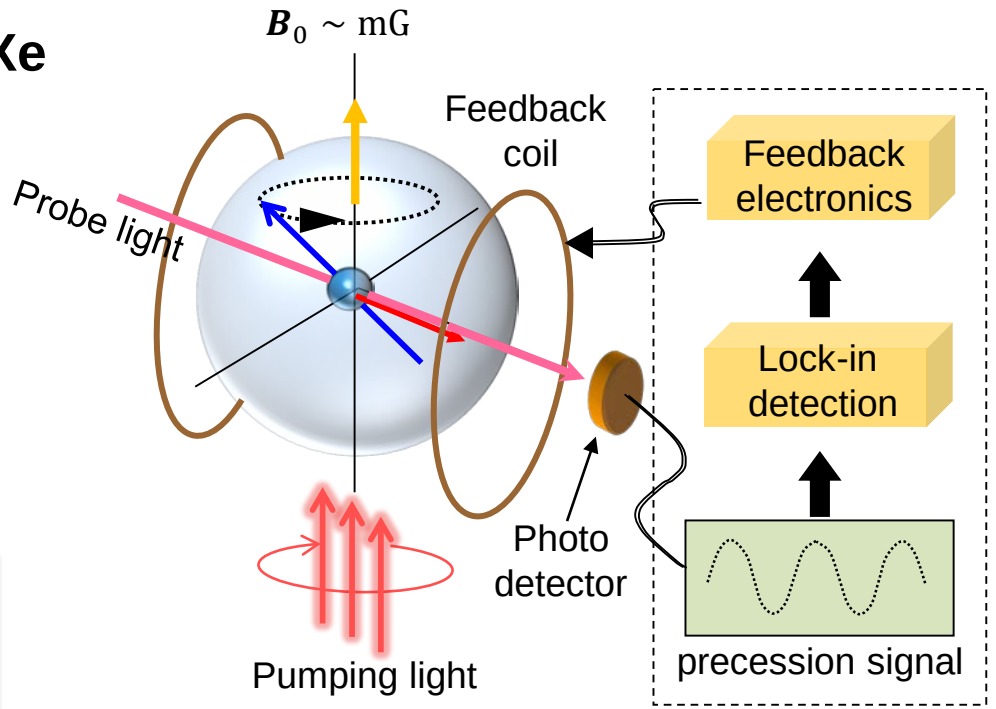

$d \sim 10^{-28}$ ecm EDM sensitivity

$\Delta\nu \sim 1$ nHz frequency precision
(@E = 10 kV/cm)

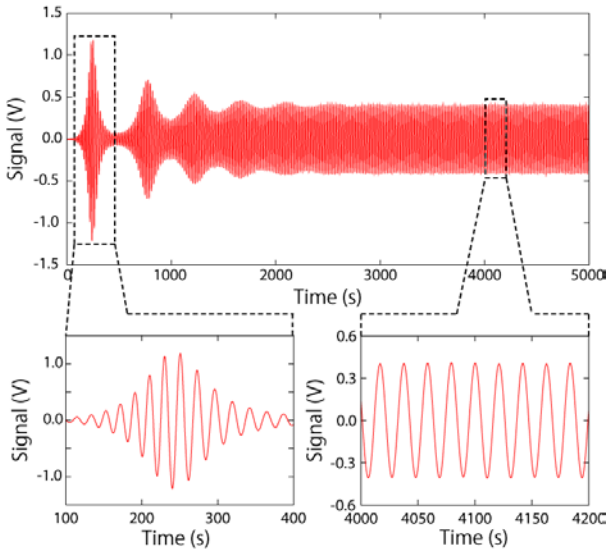

Current experimental limits:

$|d(^{129}\mathrm{Xe})| < 4.1 \times 10^{-27}$ *e*cm

M. A. Rosenberry *et al.*, Phys. Rev. Lett. 86, 22 (2001)

(c.f. $|d(^{199}\mathrm{Hg})| < 3.1 \times 10^{-29}$ *e*cm)

W. C. Griffith *et al.*, Phys. Rev. Lett. 102, 101601 (2009)

Sources of systematic errors in maser frequency

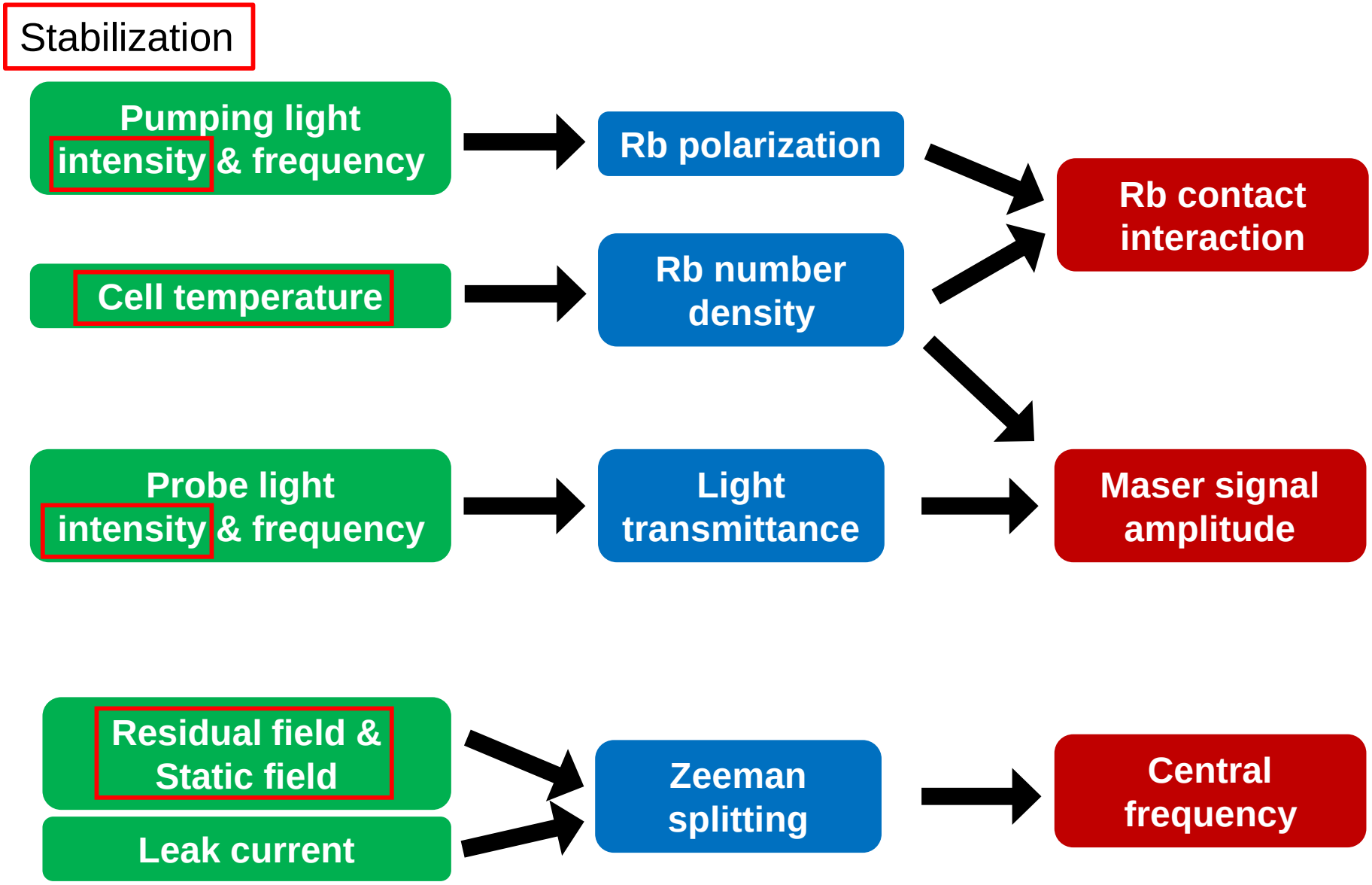

Stabilization of maser operation parameters

- Cell temperature
  - PID feedback to the heater

✓ 1/20 reduction of long-term drift
✓ ～10^{-2}℃ precision @10^4 s ave.

Temperature of cell environment

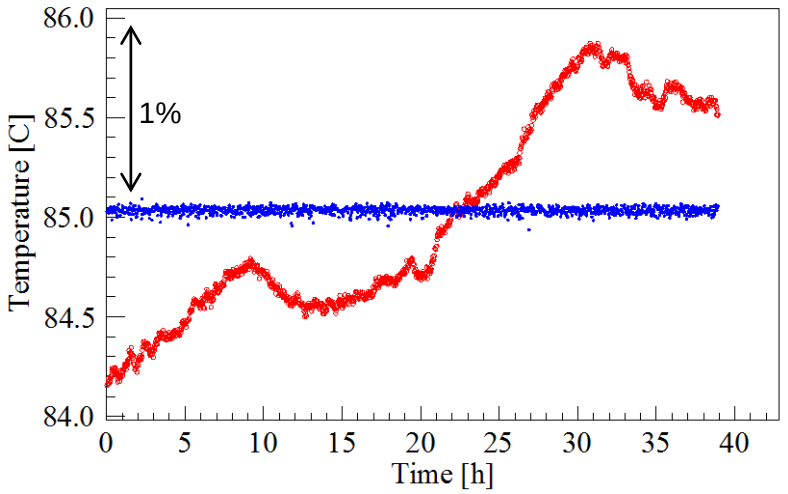

- Laser intensity
  - Stabilization feedback loop

✓ 1/10 reduction of long-term drift
✓ ～5×10^{-2}% precision @10^4 s ave.

Laser intensity monitor output

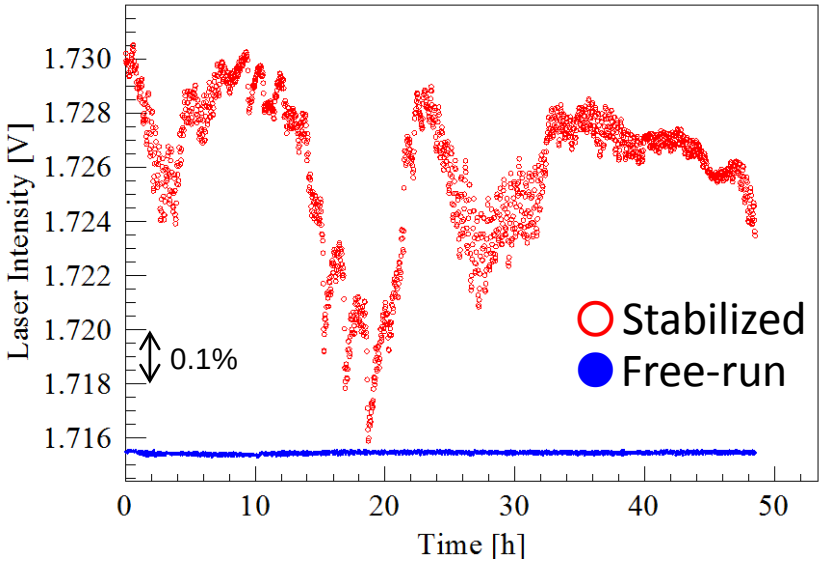

Stabilization of maser operation parameters

- Current for static field coil

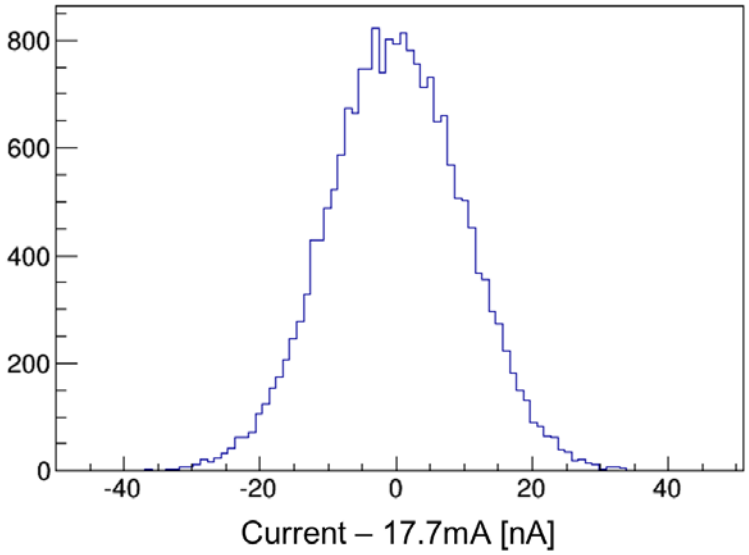

✓ 10pA precision @10^4 s ave.

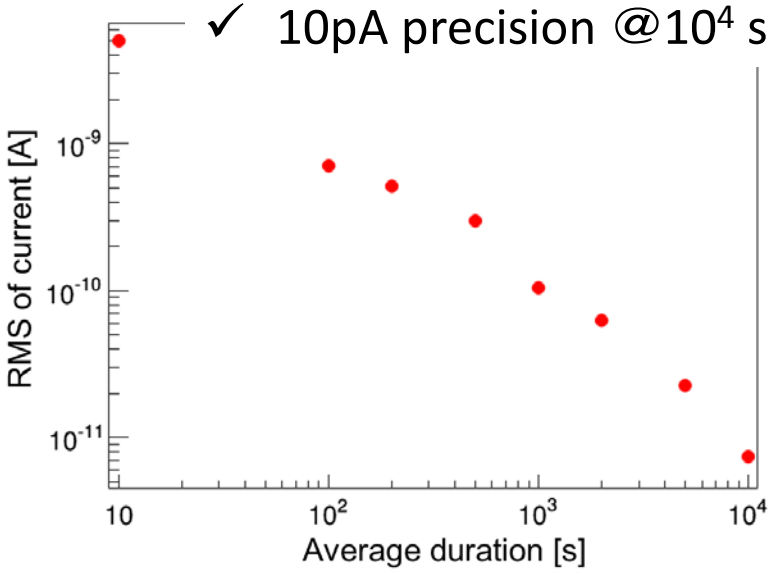

- Environmental field canceler

✓ Cancel out residual field by feedback loop

✓ Allan deviation～0.5nG @20,000s average

- Large three-layer magnetic shield

✓ 800-mmϕ × 1300 mm (Outermost layer)

✓ Shielding factor: 10^4

0.6nHz error for ^{129}Xe maser @20,000 s ave.

Sources of systematic errors in maser frequency

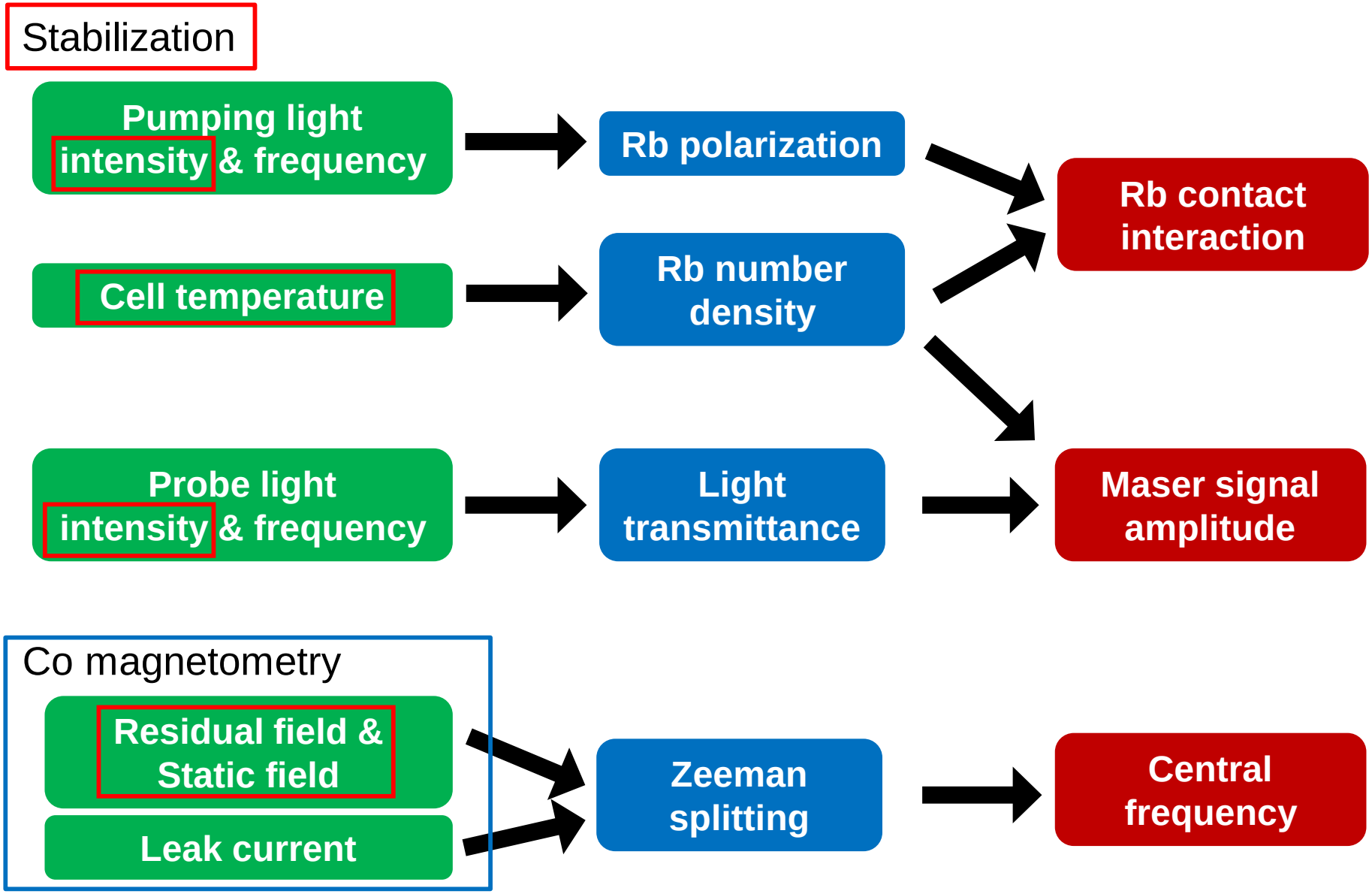

^{3}He Comagnetometry

- ^{3}He comagnetometry: cancel out the B field drift

$$\varphi_1(t) = \frac{\gamma_1}{\gamma_2} \cdot \varphi_2(t)$$

Advantage

- ✓ Nuclear spin: 1/2
- ✓ EDM: Negligible compared to ^{129}Xe

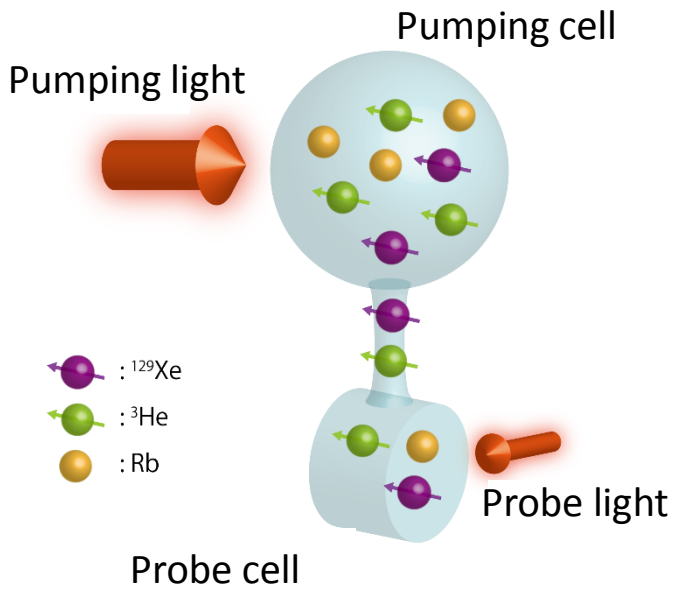

Experimental apparatus

Maser cell

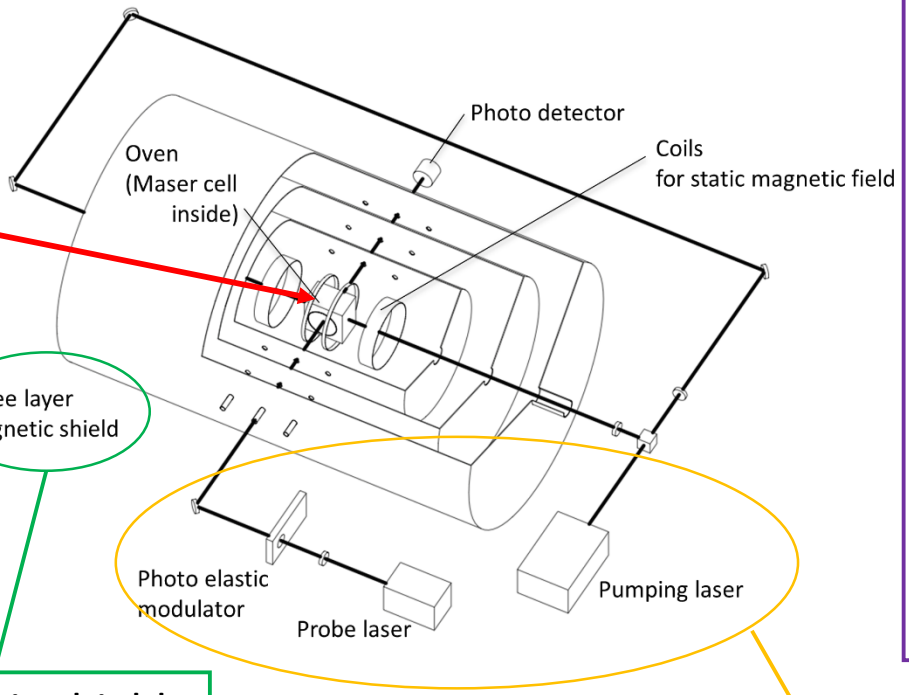

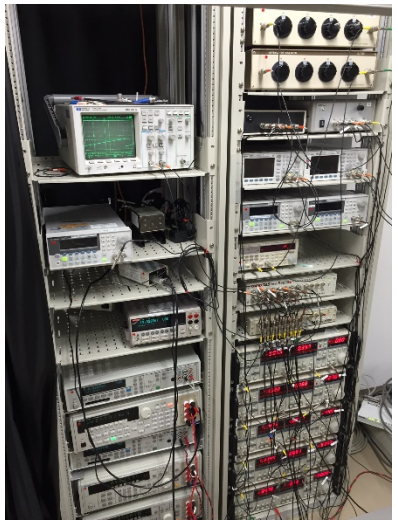

Data taking &
Feedback circuit

Large three-layer magnetic shield

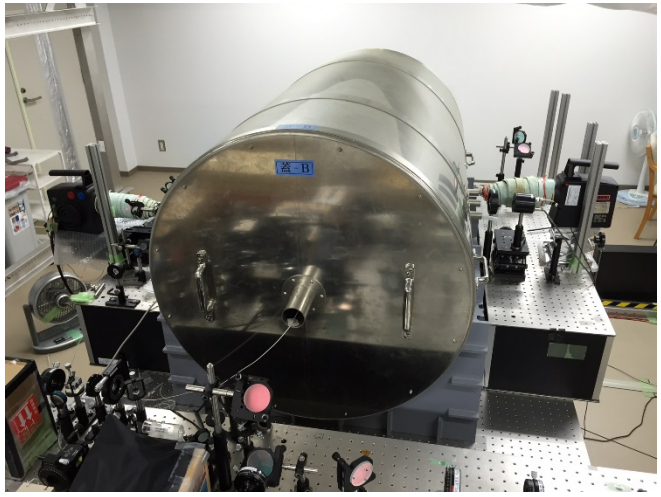

Optics

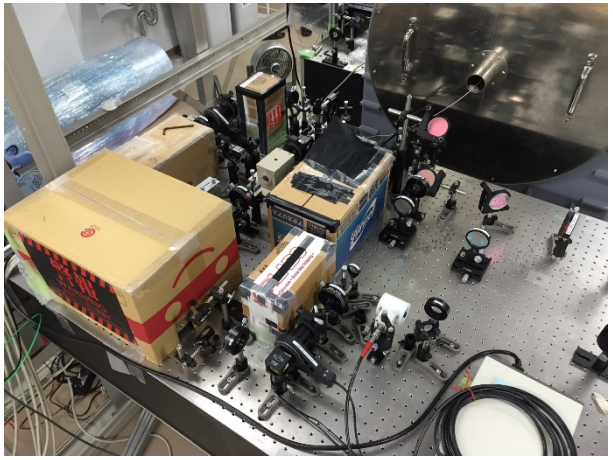

Frequency characteristics of double-cell maser

Variance of the measured maser frequency $\nu(\tau)$ as a function of the integration time τ

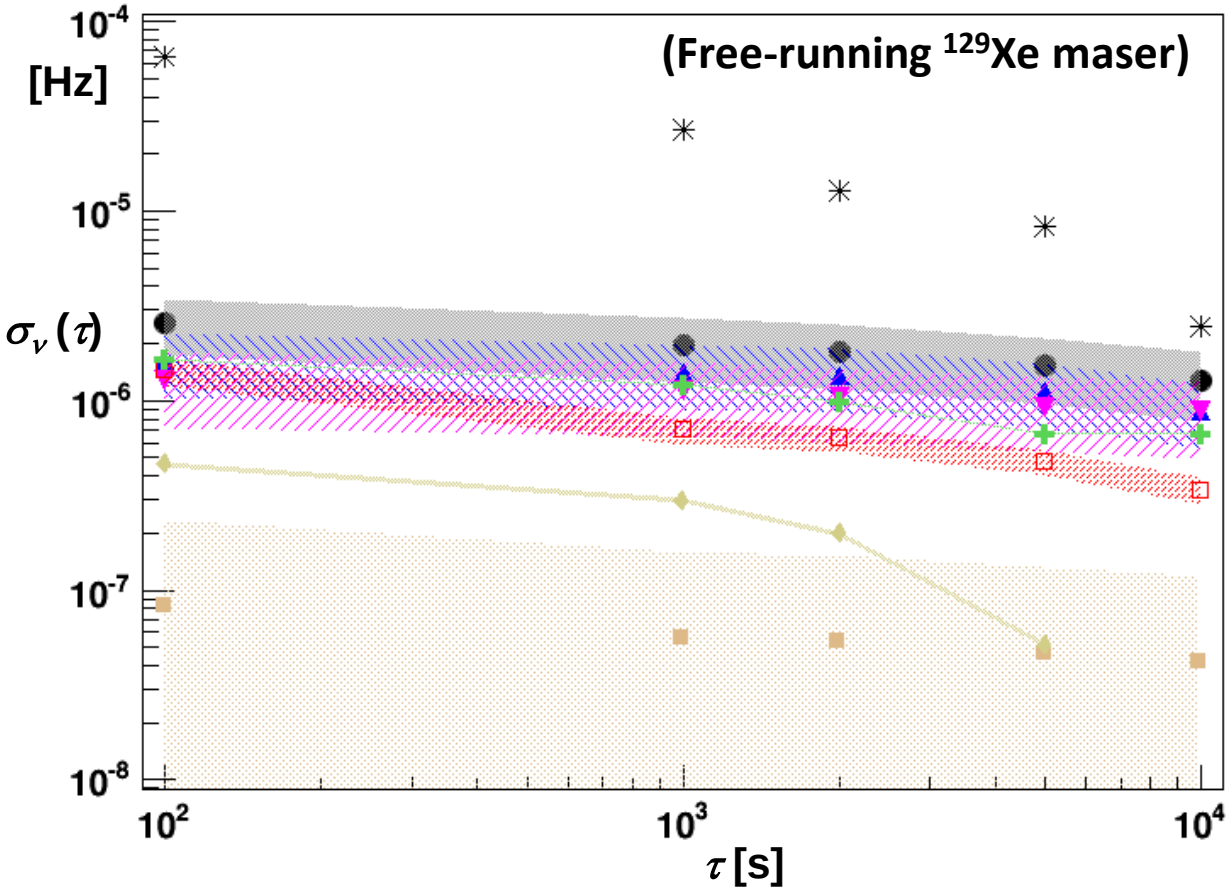

✳ **Measured ^{129}Xe maser frequency**

● **Quadrature sum of estimated errors**

Sources of frequency errors

- ▲ Probe light int.
- ▼ Pumping/ signal amp. light int.
- ✚ Pumping/ signal amp. light freq.
- □ Pumping cell temp.
- ◆ Probe light freq.
- ■ Probe cell temp.

Dominant error sources

- pumping cell temperature
- pumping/signal amp. light frequency

→ Remaining effect from pumping cell

➢ ^{3}He comagnetometry: cancel out the B field drift

$$\varphi_1(t) = \frac{\gamma_1}{\gamma_2} \cdot \varphi_2(t)$$

Advantage

- ✓ Nuclear spin: 1/2
- ✓ EDM: Negligible compared to ^{129}Xe

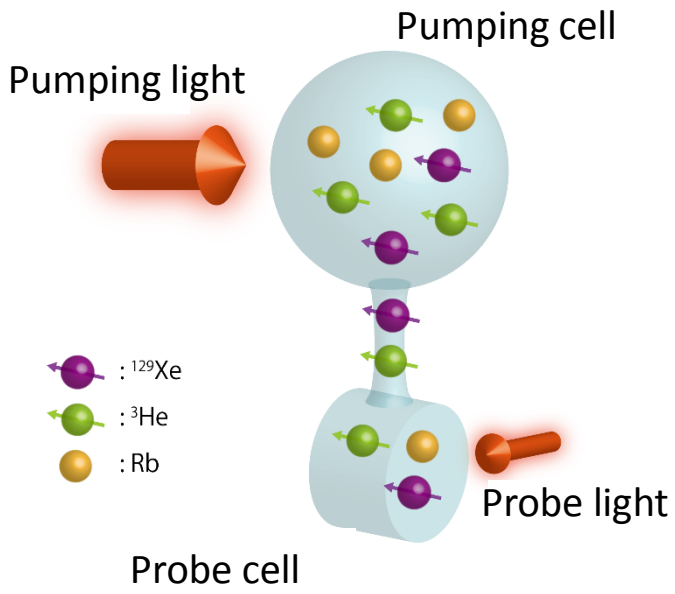

➢ ^{3}He comagnetometry: cancel out the B field drift

$$\varphi_1(t) = \frac{\gamma_1}{\gamma_2} \cdot \varphi_2(t)$$

Advantage

- ✓ Nuclear spin: 1/2
- ✓ EDM: Negligible compared to ^{129}Xe

Problem

- ✓ Contact shift associated with pol. Rb

$\Delta\nu \propto \kappa \times$ (Rb number density) $\times$ (Rb polarization)

^{129}Xe/ ^{3}He ratio～60

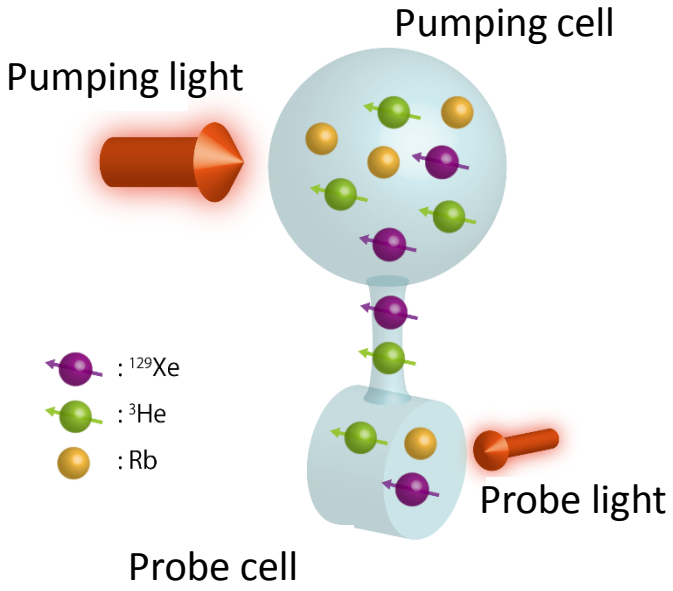

→Solution: Double-cell geometry

Suppression of P_{Rb} (Δv～1/10)

New spin maser species: ^{131}Xe

	^{3}He	^{131}Xe
Nuclear spin	1/2	3/2
EDM	Negligible to ^{129}Xe	Different for ^{129}Xe
Pol. condition	Different for ^{129}Xe	Similar to ^{129}Xe
Optical detection	Difficult	Relative easy
Pol. buildup time (T_1)	$\sim 10^4$ s	$\sim 10^2$ s
Pol. Rb shift difference	$\sim 1.3 \times 10^{-2} P_{Rb}$[Rb]	$\sim 1.7 \times 10^{-5} P_{Rb}$[Rb]
Cell geometry	Double-cell	Spherical cell

Advantages

- ✓ Suppression of pol. Rb shift
- ✓ Spherical cell geometry

Problems

- ✓ Differential measurement of EDMs
- ✓ Nuclear spin: 3/2
- ✓ Quadrupole moment

§ 3 Spin masing with *I* = 3/2 spins

$$\hat{H} = \hat{H}_{\mathrm{M}} + \hat{H}_{\mathrm{Q}}$$

where

$$\hat{H}_{\mathrm{M}} = -g\mu_{\mathrm{N}}\hat{\boldsymbol{I}}\cdot\left(\boldsymbol{B}_0 + \boldsymbol{B}_1\right)$$

$$\hat{H}_{\mathrm{Q}} = \alpha\left\{\frac{a}{2}\left[3\hat{I}_z^{\,2} - I\left(I+1\right)\right]\right.$$

$$\left. + \frac{3}{2}b\left[\hat{I}_z\left(\hat{I}_+ + \hat{I}_-\right) + \left(\hat{I}_+ + \hat{I}_-\right)\hat{I}_z\right] + \frac{3}{4}c\left(\hat{I}_+^{\,2} + \hat{I}_-^{\,2}\right)\right\}$$

where

$$\alpha \equiv \frac{e^2Qq}{4I\left(2I-1\right)},$$

$$a \equiv 3\cos^2\theta - 1,$$

$$b \equiv \sin\theta\cos\theta,$$

$$c \equiv \sin^2\theta$$

$$\omega_0 \equiv \frac{g\mu_{\mathrm{N}}B_0}{\hbar}$$

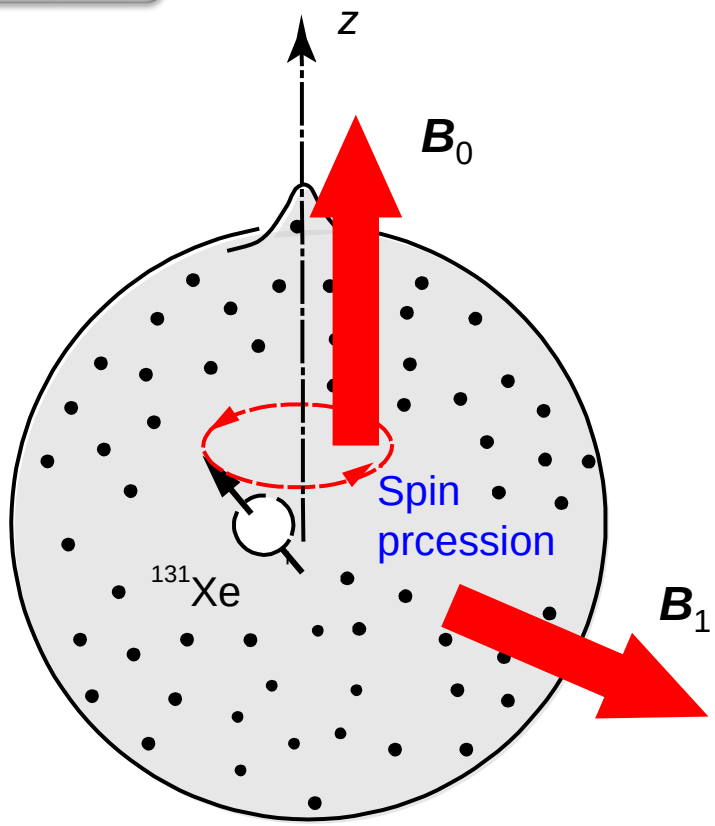

- *After a few days long cell baking, the principal axis of the electric field gradient tensor* $\boldsymbol{q}$ *is oriented in the direction of the glass tip. In this case* $\theta = 0$, *hence* $a = 1$, $b = 0$ *and* $c = 0$.

[*This part follows the discussions given by*:
T.M. Kwon *et al*, *Phys. Rev.* A **24** (1981) 1894; and
C. Cohen-Tannoudji, *J. Phys.* (Paris) **24** (1963) 653]

● To second order in H_Q, the energy eigenvalues are given, in absence of $\boldsymbol{B}_1$, as

$$E_m = E_m^{(0)} + \langle m|\hat{H}_Q|m\rangle + \sum_{m'\neq m} \frac{\left|\langle m|\hat{H}_Q|m'\rangle\right|^2}{E_m^{(0)} - E_{m'}^{(0)}}$$

and the motion of spin is described by the von Neumann equation for the density matrix

$$\hat{\rho} \equiv \sum_{m,m'} |m\rangle \rho_{mm'} \langle m'|$$

as :

$$\frac{\mathrm{d}\hat{\rho}}{\mathrm{d}t} = \frac{\mathrm{i}}{\hbar}\left[\hat{\rho}, \hat{H}\right]$$

● After switching to the interaction representation, executing the second-order time-dependent perturbation calculation and then switching back to the Schroedinger representation, we obtain the following equation of motion for ρ :

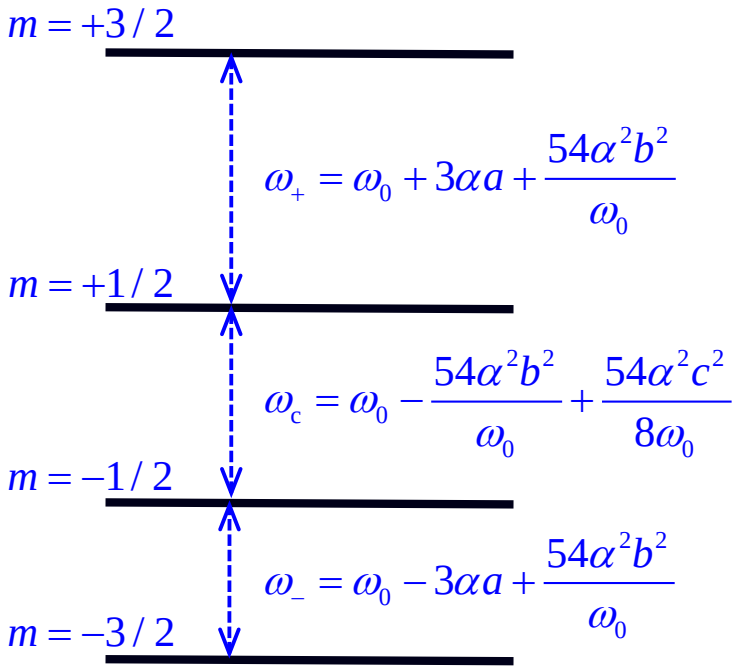

● The time evolution of the density matrix ρ

$$\frac{\mathrm{d}\hat{\rho}}{\mathrm{d}t} = \begin{pmatrix} 0 & -\omega_+\rho_{12} & -(\omega_+ + \omega_c)\rho_{13} & -(\omega_+ + \omega_c + \omega_-)\rho_{14} \\ \omega_+\rho_{21} & 0 & -\omega_c\rho_{23} & -(\omega_- + \omega_c)\rho_{24} \\ (\omega_+ + \omega_c)\rho_{31} & \omega_c\rho_{32} & 0 & -\omega_-\rho_{34} \\ (\omega_+ + \omega_c + \omega_-)\rho_{41} & (\omega_- + \omega_c)\rho_{42} & \omega_-\rho_{43} & 0 \end{pmatrix}$$

$$+\frac{1}{T_Q}\begin{pmatrix} -2\rho_{11} + \rho_{22} + \rho_{33} & -3\rho_{12} + \rho_{34} & -3\rho_{13} - \rho_{24} & -2\rho_{14} \\ -3\rho_{21} + \rho_{43} & \rho_{11} - 2\rho_{22} + \rho_{44} & -2\rho_{23} & -3\rho_{24} - \rho_{13} \\ -3\rho_{31} + \rho_{42} & -2\rho_{32} & \rho_{11} - 2\rho_{33} + \rho_{44} & -3\rho_{34} + \rho_{12} \\ -2\rho_{41} & -3\rho_{42} - \rho_{31} & -3\rho_{43} + \rho_{21} & \rho_{22} + \rho_{33} - 2\rho_{44} \end{pmatrix}$$

Then, ・・・

● The expectation values for the transverse spins $\langle \hat{I}_x \rangle$, $\langle \hat{I}_y \rangle$ are given as

$$\langle \hat{I}_x \rangle = \mathrm{Tr}(\hat{\rho}\hat{I}_x) = \underbrace{\frac{\sqrt{3}}{2}(\rho_{12} + \rho_{21})}_{\equiv M_{x1}} + \underbrace{(\rho_{23} + \rho_{32})}_{\equiv M_{x2}} + \underbrace{\frac{\sqrt{3}}{2}(\rho_{34} + \rho_{43})}_{\equiv M_{x3}} \equiv M_x$$

$$\langle \hat{I}_y \rangle = \mathrm{Tr}(\hat{\rho}\hat{I}_y) = \underbrace{\frac{\sqrt{3}}{2\mathrm{i}}(\rho_{12} - \rho_{21})}_{\equiv M_{y1}} + \underbrace{\frac{1}{\mathrm{i}}(\rho_{23} - \rho_{32})}_{\equiv M_{y2}} + \underbrace{\frac{\sqrt{3}}{2\mathrm{i}}(\rho_{34} - \rho_{43})}_{\equiv M_{y3}} \equiv M_y$$

● The time evolution of the polarization vector $\boldsymbol{M}(t)$ is

$$\frac{\mathrm{d}}{\mathrm{d}t}\begin{pmatrix} M_{x1} \\ M_{y1} \\ M_{x2} \\ M_{y2} \\ M_{x3} \\ M_{y3} \end{pmatrix} = \begin{pmatrix} -\frac{3}{T_\mathrm{Q}} - \frac{1}{T_2} & -\omega_+ & 0 & 0 & \frac{1}{T_\mathrm{Q}} & 0 \\ \omega_+ & -\frac{3}{T_\mathrm{Q}} - \frac{1}{T_2} & 0 & 0 & 0 & \frac{1}{T_\mathrm{Q}} \\ 0 & 0 & -\frac{2}{T_\mathrm{Q}} - \frac{1}{T_2} & -\omega_\mathrm{c} & 0 & 0 \\ 0 & 0 & \omega_\mathrm{c} & -\frac{2}{T_\mathrm{Q}} - \frac{1}{T_2} & 0 & 0 \\ \frac{1}{T_\mathrm{Q}} & 0 & 0 & 0 & -\frac{3}{T_\mathrm{Q}} - \frac{1}{T_2} & -\omega_- \\ 0 & \frac{1}{T_\mathrm{Q}} & 0 & 0 & \omega_- & -\frac{3}{T_\mathrm{Q}} - \frac{1}{T_2} \end{pmatrix} \begin{pmatrix} M_{x1} \\ M_{y1} \\ M_{x2} \\ M_{y2} \\ M_{x3} \\ M_{y3} \end{pmatrix}$$

● The time evolution of the polarization vector $\boldsymbol{M}(t)$ is

$$\frac{\mathrm{d}}{\mathrm{d}t}\begin{pmatrix} M_{x1} \\ M_{y1} \\ M_{x2} \\ M_{y2} \\ M_{x3} \\ M_{y3} \end{pmatrix} = \begin{pmatrix} -\frac{3}{T_\mathrm{Q}}-\frac{1}{T_2} & -\omega_+ & 0 & 0 & \cancel{\frac{1}{T_\mathrm{Q}}} & 0 \\ \omega_+ & -\frac{3}{T_\mathrm{Q}}-\frac{1}{T_2} & 0 & 0 & 0 & \cancel{\frac{1}{T_\mathrm{Q}}} \\ 0 & 0 & -\frac{2}{T_\mathrm{Q}}-\frac{1}{T_2} & -\omega_\mathrm{c} & 0 & 0 \\ 0 & 0 & \omega_\mathrm{c} & -\frac{2}{T_\mathrm{Q}}-\frac{1}{T_2} & 0 & 0 \\ \cancel{\frac{1}{T_\mathrm{Q}}} & 0 & 0 & 0 & -\frac{3}{T_\mathrm{Q}}-\frac{1}{T_2} & -\omega_- \\ 0 & \cancel{\frac{1}{T_\mathrm{Q}}} & 0 & 0 & \omega_- & -\frac{3}{T_\mathrm{Q}}-\frac{1}{T_2} \end{pmatrix} \begin{pmatrix} M_{x1} \\ M_{y1} \\ M_{x2} \\ M_{y2} \\ M_{x3} \\ M_{y3} \end{pmatrix}$$

● The time evolution of the polarization vector $\boldsymbol{M}(t)$ is

$$\frac{\mathrm{d}}{\mathrm{d}t}\begin{pmatrix} M_{x1} \\ M_{y1} \\ M_{x2} \\ M_{y2} \\ M_{x3} \\ M_{y3} \end{pmatrix} = \begin{pmatrix} -\frac{3}{T_\mathrm{Q}}-\frac{1}{T_2} & -\omega_+ & 0 & 0 & \cancel{\frac{1}{T_\mathrm{Q}}} & 0 \\ \omega_+ & -\frac{3}{T_\mathrm{Q}}-\frac{1}{T_2} & 0 & 0 & 0 & \cancel{\frac{1}{T_\mathrm{Q}}} \\ 0 & 0 & -\frac{2}{T_\mathrm{Q}}-\frac{1}{T_2} & -\omega_\mathrm{c} & 0 & 0 \\ 0 & 0 & \omega_\mathrm{c} & -\frac{2}{T_\mathrm{Q}}-\frac{1}{T_2} & 0 & 0 \\ \cancel{\frac{1}{T_\mathrm{Q}}} & 0 & 0 & 0 & -\frac{3}{T_\mathrm{Q}}-\frac{1}{T_2} & -\omega_- \\ 0 & \cancel{\frac{1}{T_\mathrm{Q}}} & 0 & 0 & \omega_- & -\frac{3}{T_\mathrm{Q}}-\frac{1}{T_2} \end{pmatrix} \begin{pmatrix} M_{x1} \\ M_{y1} \\ M_{x2} \\ M_{y2} \\ M_{x3} \\ M_{y3} \end{pmatrix}$$

$$\begin{cases} \dfrac{\mathrm{d}}{\mathrm{d}t}\boldsymbol{M}_1 = \boldsymbol{\omega}_+ \times \boldsymbol{M}_1 - \dfrac{1}{T_2^*}\boldsymbol{M}_1 & \left(\dfrac{1}{T_2^*} \equiv \dfrac{1}{T_2} + \dfrac{3}{T_\mathrm{Q}}\right) \\ \dfrac{\mathrm{d}}{\mathrm{d}t}\boldsymbol{M}_2 = \boldsymbol{\omega}_\mathrm{c} \times \boldsymbol{M}_2 - \dfrac{1}{T_2^*}\boldsymbol{M}_2 & \left(\dfrac{1}{T_2^*} \equiv \dfrac{1}{T_2} + \dfrac{2}{T_\mathrm{Q}}\right) \\ \dfrac{\mathrm{d}}{\mathrm{d}t}\boldsymbol{M}_3 = \boldsymbol{\omega}_- \times \boldsymbol{M}_3 - \dfrac{1}{T_2^*}\boldsymbol{M}_3 & \left(\dfrac{1}{T_2^*} \equiv \dfrac{1}{T_2} + \dfrac{3}{T_\mathrm{Q}}\right) \end{cases}$$

The Bloch equations for three independent S=1/2 spin systems !

External-feedback spin maser

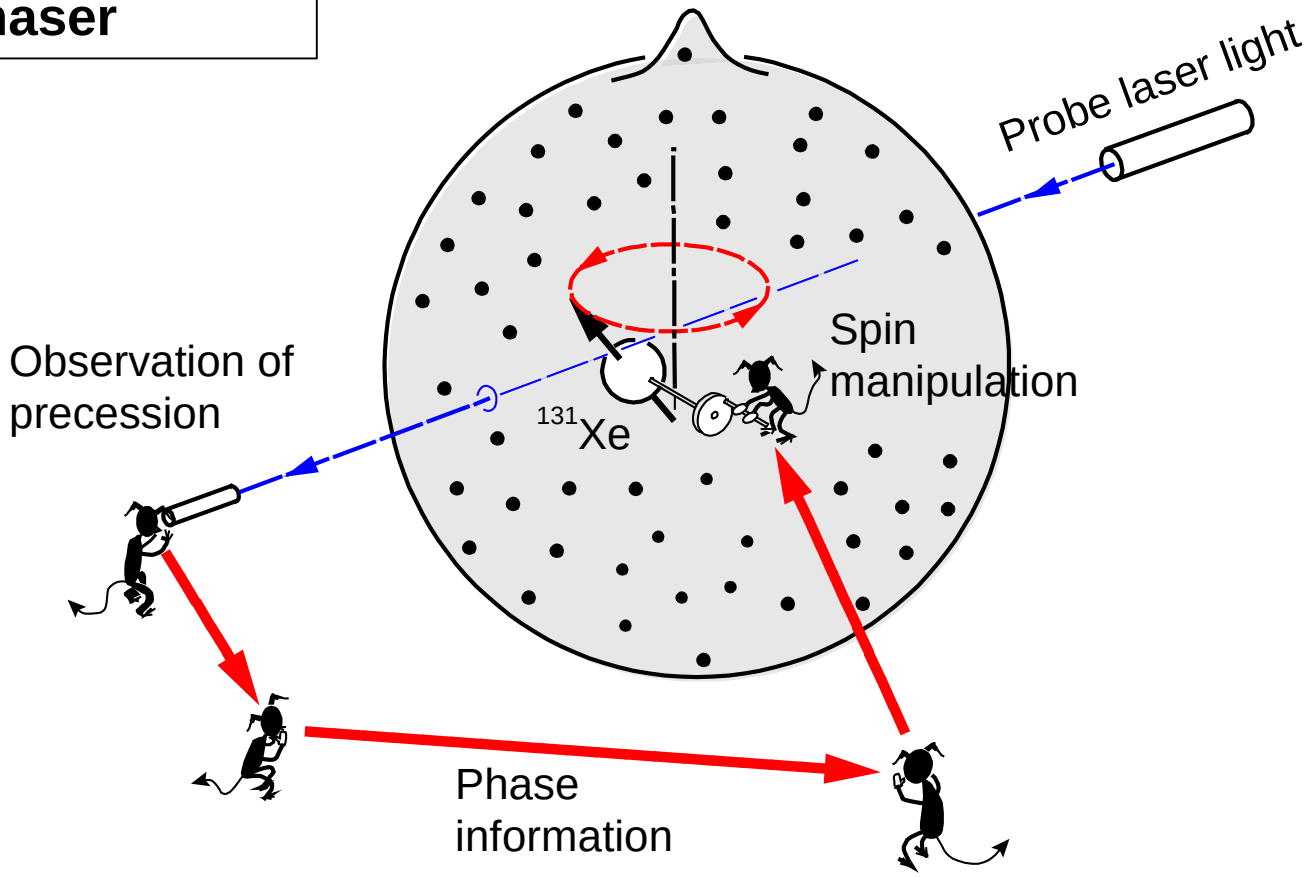

Thus, a spin maser of the *I* = 3/2 spin of ^{131}Xe atom should work!

§ 4 Present status

AFP-NMR signals

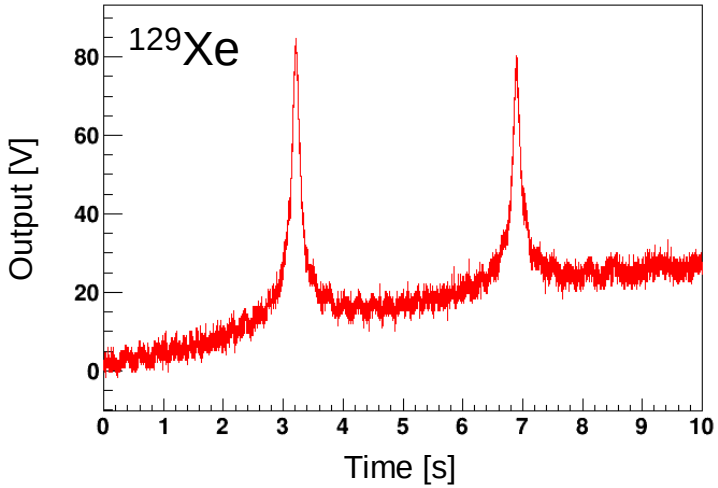

^{131}Xe polarization and relaxation

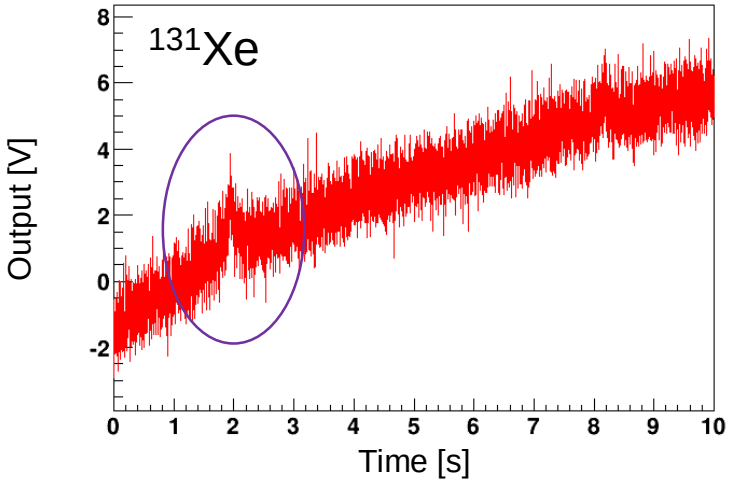

T_1 measurement

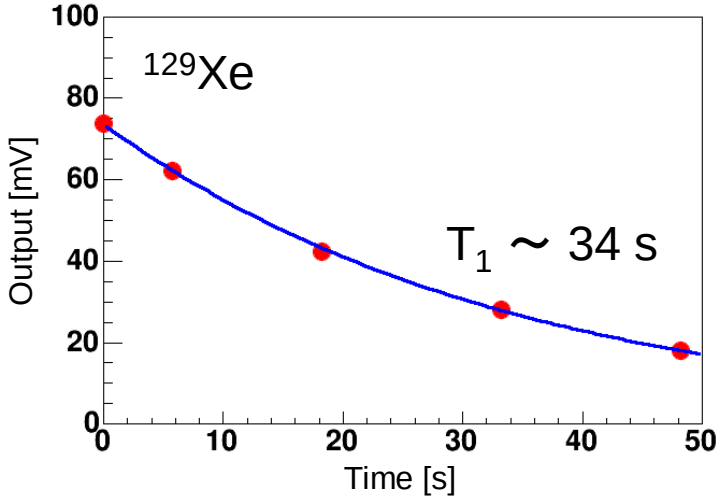

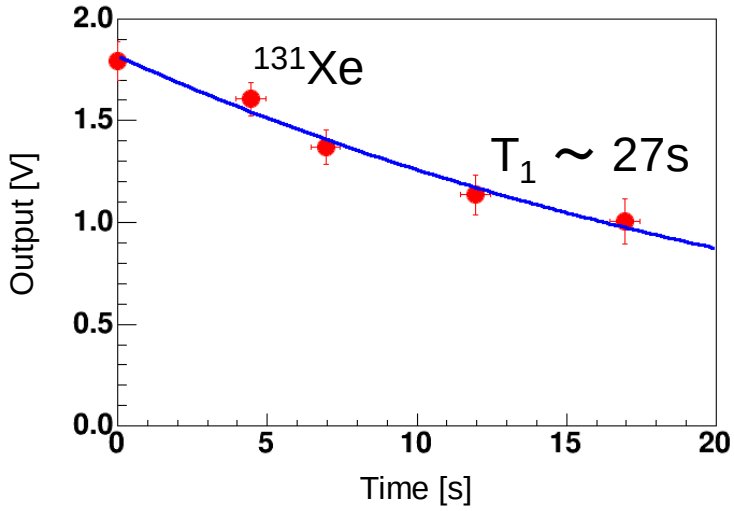

Observation of ^{129}Xe /^{131}Xe dual maser oscillation

Nuclear spin maser with *I* =3/2 system: Is it ~~possible~~? Possible!

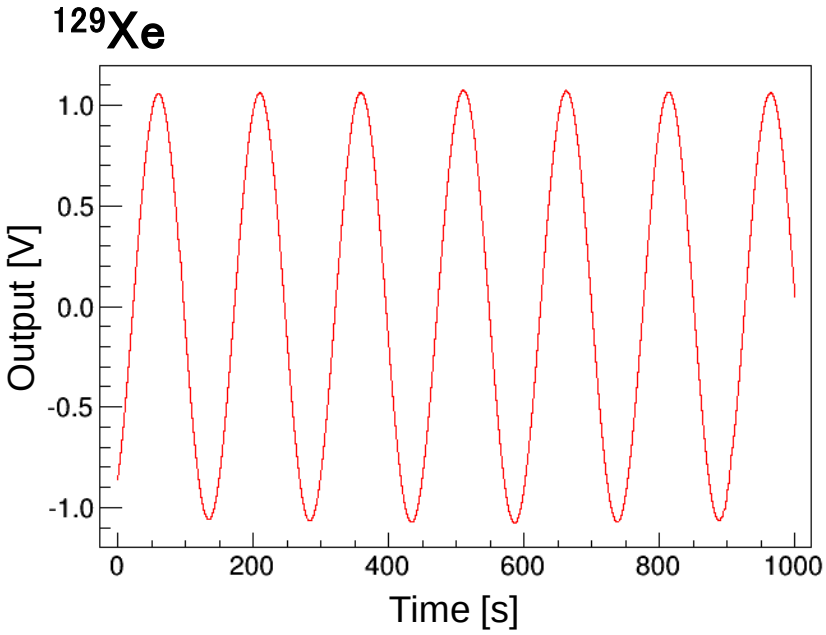

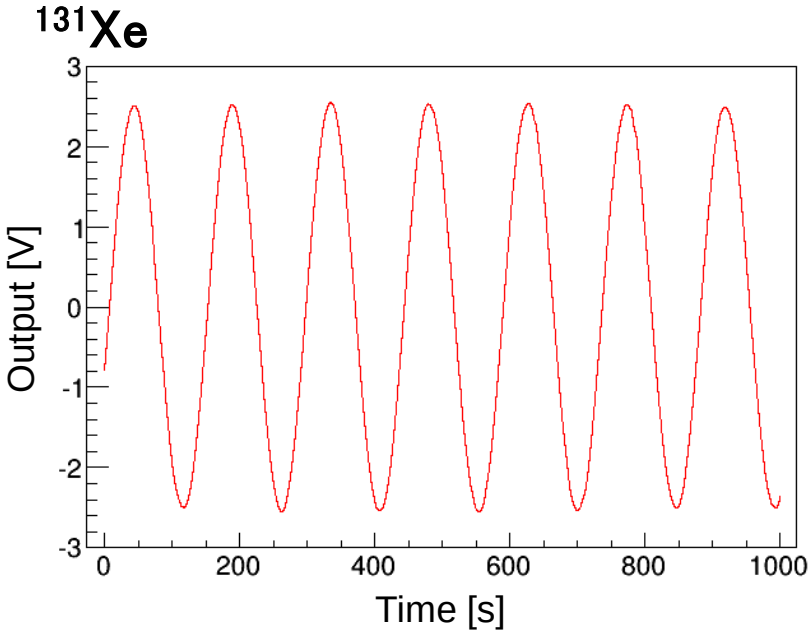

^{129}Xe/^{131}Xe maser oscillation with spherical cell successfully observed

Study of ^{129}Xe /^{131}Xe maser behaver

Response for

- Magnetic field
- Cell temperature
- Probe light intensity & frequency
- Pumping light intensity & frequency are measured

ex.) Maser response for probe & pumping light frequency

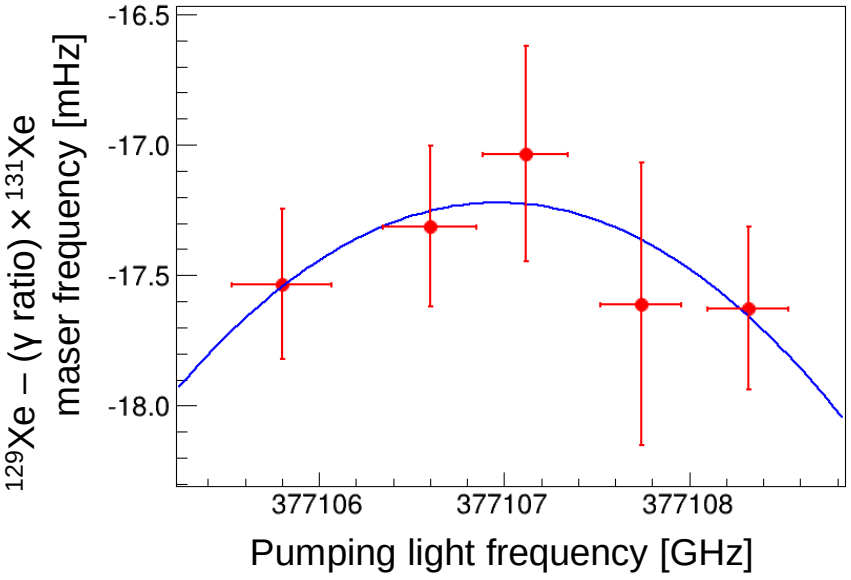

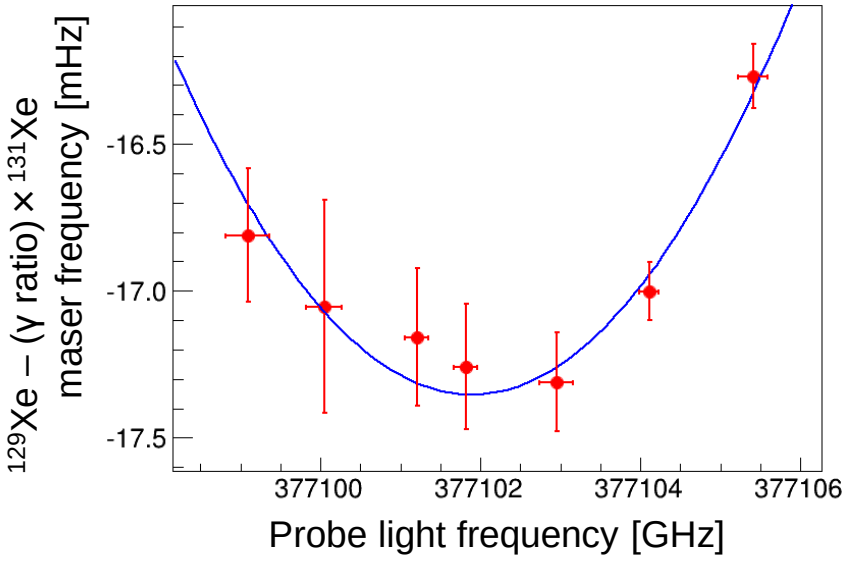

Expected maser frequency precision

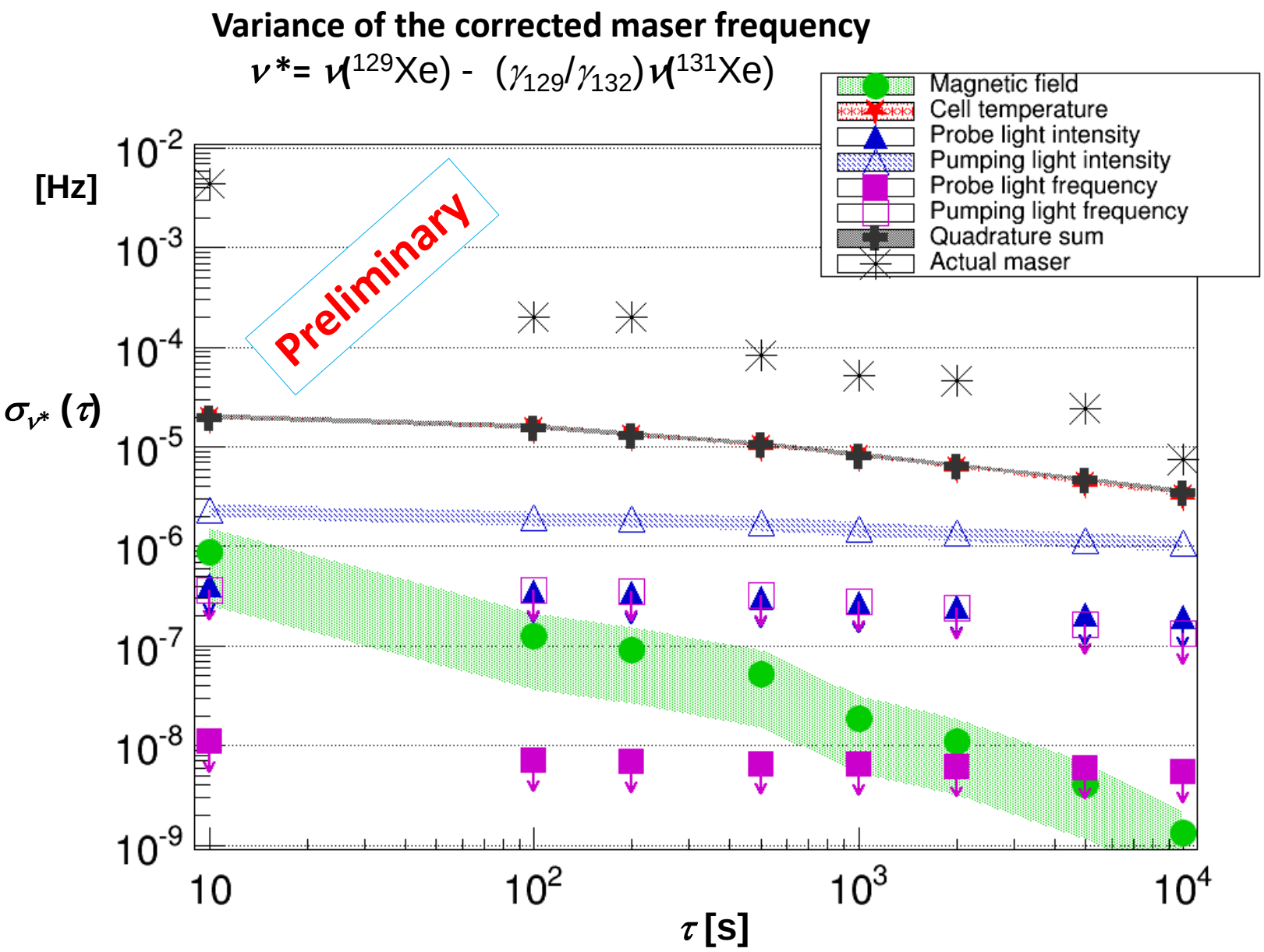

SUMMARY

- EDMs in diamagnetic atoms and neutron are indispensable sources of information on

$$C_{\mathrm{T}},\ \bar{g}^{(0)}_{\pi\mathrm{NN}},\ \bar{g}^{(1)}_{\pi\,\mathrm{NN}}$$

  among the seven experimentally accessible global parameters

$$d_{\mathrm{e}},\ C_{\mathrm{S}},\ C_{\mathrm{T}},\ \bar{g}^{(0)}_{\pi\mathrm{NN}},\ \bar{g}^{(1)}_{\pi\,\mathrm{NN}},\ \bar{d}^{\mathrm{sr}}_{\mathrm{n}},\ \bar{d}^{\mathrm{sr}}_{\mathrm{p}}$$

  that can appear in low energy particles, as evidences for the presence of fundamental theory beyond the Standard Model.

- Xe EDM could play a crucial role in separating the combined contributions $C_{\mathrm{T}} + \bar{g}^{(0)}_{\pi\mathrm{NN}} + \bar{g}^{(1)}_{\pi\,\mathrm{NN}}$

- In order to detect ^{129}Xe EDM, a neighboring odd-mass isotope ^{131}Xe, though its spin is 3/2, would provide a useful co-magnetometry.

- Double-species spin maser of ^{129}Xe and ^{131}Xe has been successfully operated and its frequency stability is currently being studied.

Backup slides

● The time evolution of the density matrix ρ

$$\frac{\mathrm{d}\hat{\rho}}{\mathrm{d}t} = \begin{pmatrix} 0 & -\omega_+\rho_{12} & -(\omega_+ + \omega_\mathrm{c})\rho_{13} & -(\omega_+ + \omega_\mathrm{c} + \omega_-)\rho_{14} \\ \omega_+\rho_{21} & 0 & -\omega_\mathrm{c}\rho_{23} & -(\omega_- + \omega_\mathrm{c})\rho_{24} \\ (\omega_+ + \omega_\mathrm{c})\rho_{31} & \omega_\mathrm{c}\rho_{32} & 0 & -\omega_-\rho_{34} \\ (\omega_+ + \omega_\mathrm{c} + \omega_-)\rho_{41} & (\omega_- + \omega_\mathrm{c})\rho_{42} & \omega_-\rho_{43} & 0 \end{pmatrix}$$

$$+\frac{1}{T_\mathrm{Q}}\begin{pmatrix} -2\rho_{11}+\rho_{22}+\rho_{33} & -3\rho_{12}+\rho_{34} & -3\rho_{13}-\rho_{24} & -2\rho_{14} \\ -3\rho_{21}+\rho_{43} & \rho_{11}-2\rho_{22}+\rho_{44} & -2\rho_{23} & -3\rho_{24}-\rho_{13} \\ -3\rho_{31}+\rho_{42} & -2\rho_{32} & \rho_{11}-2\rho_{33}+\rho_{44} & -3\rho_{34}+\rho_{12} \\ -2\rho_{41} & -3\rho_{42}-\rho_{31} & -3\rho_{43}+\rho_{21} & \rho_{22}+\rho_{33}-2\rho_{44} \end{pmatrix}$$

where the relaxation arises from the second term, with

$$\frac{1}{T_\mathrm{Q}} = \frac{36\pi}{5}\frac{\tau_\mathrm{s}}{\tau_\mathrm{s}+\tau_\mathrm{v}}\left(\frac{e^2qQ}{3}\right)^2\tau_\mathrm{c}$$

Here τ_s, τ_v, τ_c are estimated in [Kwon 1981] as

$\tau_\mathrm{s} \sim 6.6\times10^{-11}$ s (sticking time on the wall)

$\tau_\mathrm{v} \sim 3.5\times10^{-3}$ s (time between wall collisions)

$\tau_\mathrm{c} \sim 3.5\times10^{-7}$ s (correlation time for the wall quadrupole interaction)